50-322 OL

I-SC-7
I-SC-10
I-SC-35 through
I-SC-39 10/1/84

SUFFOLK COUNTY, 7/31/84

UNITED STATES OF AMERICA
NUCLEAR REGULATORY COMMISSION

Before the Atomic Safety and Licensing Board

In the Matter of	)	
	)	
LONG ISLAND LIGHTING COMPANY	)	Docket No. 50-322-OL
	)	
(Shoreham Nuclear Power Plant, Unit 1).	)	
	)	

SUFFOLK COUNTY'S EXHIBITS TO JOINT DIRECT TESTIMONY

~~CURRICULA VITAE~~

CRANKSHAFT EXHIBITS
7, 10, 35-39
VOLUME 1

NUCLEAR REGULATORY COMMISSION

Docket No. 50-322 Official Exh. No. 7, 10, 35-39
In the matter of LILCO
Staff IDENTIFIED ✓
Applicant RECEIVED ✓
Intervenor ✓ REJECTED
Con'g Ofcr.
Contractor DATE 10-1-84
Other COUNTY'S Witness
Reporter L.A.B.

UNITED STATES OF AMERICA
NUCLEAR REGULATORY COMMISSION

Before the Atomic Safety and Licensing Board

In the Matter of	)	
LONG ISLAND LIGHTING COMPANY	)	Docket No. 50-322-OL
(Shoreham Nuclear Power Plant, Unit 1).	)	

INDEX TO THE ATTACHMENTS AND EXHIBITS TO THE JOINT DIRECT TESTIMONY OF DR. ROBERT N. ANDERSON, PROFESSOR STANLEY G. CHRISTENSEN, G. DENNIS ELEY, DALE G. BRIDENBAUGH AND RICHARD B. HUBBARD REGARDING SUFFOLK COUNTY'S EMERGENCY DIESEL GENERATOR CONTENTIONS

VOLUME 1
CRANKSHAFT EXHIBITS 7, 10, 35-39

7. Design Review of TDI R-4 and RV-4 Series Emergency Diesel Generator Cylinder Blocks and Liners, June 1984

10. Deposition of Gerald Edgar Trussell, pgs. 62, 45-48, 107, 111-113

35. Board Notification 84-101 - Crankshaft Failure 1-6, 33-34, 59-62, 63-68,

36. Christensen's Preliminary Calculations for 12 x 13" Crankshafts Under Lloyds Register Rules

37. Lloyds Rules for Crankshafts

38. IACS - CIMAC Rules for the Calculation of Crankshafts for Diesel Engines

39. TDI Memo on IACS-CIMAC Rules on R-48 Crankshaft

FaAA-84-5-4
03315A/RKT

DESIGN REVIEW OF TDI R-4 AND RV-4 SERIES EMERGENCY DIESEL GENERATOR CYLINDER BLOCKS AND LINERS

****

This report is final, pending confirmatory reviews
required by FaAA's QA operating procedures.

****

Prepared by
Failure Analysis Associates
Palo Alto, California

Prepared for

TDI Diesel Generator Owners Group

June 1984

STATEMENT OF APPLICABILITY

This report summarizes a structural integrity investigation of the TDI R-4 and RV-4 series engines installed in emergency generator sets in nuclear power stations.

EXECUTIVE SUMMARY

This report summarizes a generic investigation of the structural adequacy of the TDI R-4 and RV-4 series diesel engine blocks. The results are based on strain gage testing; analytical models, including several 2-D finite element analyses; and review of field experience.

Cracks in the block top region have been identified in the diesel generator engines at Shoreham Nuclear Power Station (SNPS) and in other engines in non-nuclear service. The majority of cracks can be classified either as radial cracks, extending in a vertical plane outward from the cylinder head stud counterbore, or as circumferential cracks, extending downward from a horizontal plane and outward from the corner of the cylinder liner landing. The radial cracks are the only type found in the SNPS engines, but both radial and circumferential cracks have been found elsewhere in non-nuclear service.

An additional type of cracking identified at SNPS is associated with the camshaft bearing supports. This cracking is unique to the inline engines and is attributed by FaAA to the casting process. At Comanche Peak, cracks unique to one engine block have been found. These have also been attributed by FaAA to the casting process.

There are three possible mechanisms of crack initiation (acting separately or in combination) in the block top. The first mechanism is low cycle fatigue (LCF) associated with the stress range from each startup to high load levels. The second is high frequency fatigue (HFF) due to the firing pressure stresses. For both LCF and HFF there is a high mean tensile stress resulting from thermal expansion and stud preloading. The sum of mean and alternating components may produce the third mechanism, overload rupture. This is most likely to occur above rated power level (>110%) in blocks with below average material properties.

All of the three mechanisms are potentially responsible for initiating cracks in the ligaments between the cylinder head stud holes and the liner counterbore, and such cracking is predicted to occur by Goodman diagram analysis. The only projected consequences of this ligament cracking are possible

coolant leakage (but not into the cylinder) and greater chance of cracking between studs of adjacent cylinders. Ligament cracks alone do not appear to affect the operation or availability of the engine, as shown by field experience.

Cracking between stud holes of adjacent cylinders has been observed infrequently, but is potentially more serious than ligament cracking. This cracking has been observed in SNPS engine DG103 to a depth of 5 $^{1}/_{2}$ inches. No adverse consequences to engine operation were experienced. Cracking between stud holes is conservatively predicted by Goodman diagram fatigue analysis, assuming a ligament to be cracked, either in LCF or HFF.

A linear cumulative damage model and the observed crack growth in SNPS engine DG103 were combined to predict conservatively the amount of crack propagation that might occur during one LOOP/LOCA event. This analysis indicates that blocks with ligament cracks (e.g., DG101 and DG102) are predicted to withstand a LOOP/LOCA event with sufficient margin provided that: (1) inspection shows no stud-to-stud cracks detectable between heads, and (2) the specific block material of DG103 is shown to be sufficiently less resistant to fatigue than typical gray cast iron, Class 40.

The block tops of all engines that have operated at or above rated load should be inspected for ligament cracks. Engines such as those at Catawba and Grand Gulf that are found to be without ligament cracks can be operated without additional inspection for combinations of load, time, and number of starts that produce less expected damage than the cumulative damage prior to the latest inspection. Engines that have been operated at or above rated load without subsequent inspection of the block top should conservatively be assumed to have cracked ligaments for the purpose of defining inspection intervals.

For blocks with known or assumed ligament cracks the basic approach to assuring reliability is inspection and material evaluation. The absence of detectable cracks between stud holes should be established by eddy current inspection between heads and at the ends of the block before returning the engine to emergency standby service after any period of operation other than

no load. If crack indications are found, removal of the adjacent heads and detailed inspection and evaluation of the block top are necessary. In addition, it is necessary to ensure that the microstructure of the block top does not indicate inferior mechanical properties.

Engines that operate at lower maximum pressure and temperature than the SNPS engines (e.g., San Onofre) may have increased margins against block cracking that could allow relaxation of block top inspection requirements. Modifications such as increased liner-to-block radial clearance or avoidance of loads above 100% of rated power will reduce stresses, and site specific analyses of such modifications could also permit relaxation of inspection requirements. As additional field data, plant-specific analyses, and results from additional testing become available, it is expected that these conservative recommendations will be relaxed except for blocks in which chemistry or microstructure are indicative of lower strength.

TABLE OF CONTENTS

1.0 INTRODUCTION

This report presents a generic analysis of structural integrity of cylinder blocks and liners for TDI R-4 and RV-4 series diesel engines. The integrity of any particular cylinder block depends upon several plant-specific variables such as firing pressure and temperature, assembly clearances, cylinder head stud configuration, and material properties.

1.1 Service Experience

Two types of cracks have been found to occur in cylinder block tops of this design: cracks in the radial/vertical plane at the stud holes, and circumferential cracks in the liner counterbore at the liner landing ledge [1-1]. Figure 1-1 depicts the potential location of block top radial and circumferential cracks. In addition, for the in-line engines, cracks have occurred in the cam gallery above the cam shaft bearing supports. The survey of industry experience with TDI R-4 and RV-4 engines summarized in this section has not been independently confirmed by FaAA, and therefore is not subject to FaAA's usual quality assurance procedures.

1.1.1 Shoreham Nuclear Power Station

Shoreham has three TDI DSR-48 diesel engines designated DG101, DG102, and DG103. As of April 30, 1984, the engines had operated between 1091 and 1270 hours. A significant percentage of those hours was at or above full load, as shown by Tables 1-1 through 1-3.

As part of the engine requalification program after the crankshaft replacement, each engine was operated for 100 hours at or above full load and was then disassembled and inspected. During these inspections, radial/vertical cracks were discovered in the blocks of all three engines. Crack maps for DG101, DG102, and DG103 are presented in Figures 1-2, 1-3, and 1-4, respectively.

No circumferential cracks were found in any of the engines. However, each block had radial/vertical cracks between the cylinder bore and the stud hole. Sixty-seven percent of the ligament cracks were between 1 and 1 $^1/_2$ inches deep. A typical example of a cross-section of a radial/vertical crack through a ligament is shown in Figure 1-5. As depicted in the figure, none of the cracks extended below the corner formed by the counterbore and the counterbore landing. This demonstrates the apparent arrest of radial/vertical cracks that occur in the ligament region. In addition, when first inspected, the engine block from DG103 had a crack that extended between two adjacent studs on the exhaust side of Cylinder Nos. 4 and 5 as shown in Figure 1-6.

After inspection, DG102 was operated through 100 starts to loads greater than 50% and was then reinspected. Review of inspection reports before and after the 100 starts showed no crack extension discernable by eddy current examination of the stud holes and liner counter bores.

In order to allow calculation of the growth rate for the crack between stud holes in the DG103 block, a strain gage test of the block top was performed, as described in Section 3.0. After the strain gage test, LILCO continued with qualification testing of the DG103 engine. While operating the engine at full load, the plant experienced an abnormal load excursion. During this event, the power demand exceeded the diesel capacity and, over a period of 23 seconds, the diesel slowed to around 390 rpm, at which time the load was dropped. The diesel continued to run at low load for 10 minutes before it was manually shut off. Upon restarting the engine and continuing with qualification testing at 3900 kW, a crack at Cylinder No. 1 was noticed, and the testing was stopped. At the time the crack was noticed it was reported that the engine output parameters were satisfactory.

Inspection of the block top revealed cracks between stud holes with depth of 1 $^1/_2$ inches similar to those shown in Figure 1-6 at three locations. At four other locations, between-stud cracks developed along the top surface which did not extend to measureable depths down the sides of the stud hole. At one location a crack that previously extended 0.8 inch radially from one stud hole towards the adjacent stud hole grew to a maximum depth of 3.9 inches. In addition, the original crack between Cylinder Nos. 4 and 5 had ex-

tended to a depth of at least 5 $^{1}/_{2}$ inches. As shown in Figure 1-7, the ligament cracks had also grown approximately 1 inch. Figure 1-8 is a crack map for DG103 as reinspected.

1.1.2 Inspection of Blocks at Other Nuclear Power Stations

Catawba Nuclear Power Station has operated its 1a emergency diesel generator approximately 810 hours. The 1a diesel has been inspected for block top cracks, and none have been found. The load history for the 1a engine is shown in Table 1-4.

River Bend has two TDI diesel engines of the DSR-48 design. Each engine has approximately 50 hours of factory operation only. Engine logs show that both engines were run at 100% load. To date one engine block has been inspected by the magnetic particle method. No cracks were found in the block top.

Comanche Peak Steam Electric Station has inspected both of its TDI DSRV-16-4 engines. The engines have been operated for approximately 90 hours at the site. Subsequent inspection of the block top region revealed several indications that are considerably different from radial/vertical cracks found at SNPS or elsewhere. The two largest indications, illustrated in Figure 1-1, have been metallurgically examined and were identified as interdendritic shrinkage or porosity resulting from the casting process.

Grand Gulf Nuclear Station has inspected the block top of the Division 1 engine after 1,397 hours of operation, including 338 hours between 80% and 100% load, and 14 hours at 110% load since November 1981 [1-2]. No indications were reported. The load history is shown in Table 1-4.

1.1.3 Non-Nuclear Service

The experience compiled for engines in non-nuclear service tends to support the observation of the apparent arrest of ligament cracks at the depth of the liner landing ledge ($1^{1}/_{2}$ inches) when cracks between stud holes are not present. The motor vessel Edwin H. Gott has been operating for at least

7500 hours with cracks of this type [1-3]. The crack depth has been monitored at intervals of six months. According to the operators of the vessel, no crack growth has been detected over this period of operation.

The motor vessel Columbia had operated for 30,000 hours at the time cylinder block cracks were identified [1-1]. Both types of cracks were present.

A block from a dual-fuel V-16 engine (the St. Cloud block at TDI in Oakland) shows extensive radial and circumferential cracks. Several radial cracks appear between stud holes without ligament cracks. The cracks are shown in Figures 1-9 and 1-10, but depths are not available. The detailed operating history of this block is unknown, but it had over 16,000 hours in municipal power service with fuels of varying heat content. Detonation of the gaseous fuel mixture is believed to have occurred in service, causing increases in cylinder pressure on the order of a factor of two.

The Copper Valley Electric Association has been operating DSR-46 engines (two in Valdez, Alaska, and two in Glennallen, Alaska) for four years with known ligament cracks. These plants both run continuously to provide electrical power to local consumers and, therefore, it is reasonable to believe that the individual engines have gathered in excess of 28,000 operating hours with these cracks [1-4].

The City of Homestead, Florida has run each of its two DSRV-20-4 TDI engines more than 6,000 operating hours with ligament cracks [1-5].

The motor vessels Traveller and Trader operated by Biehl Offshore, Inc., are known to have ligament cracks that were reportedly first noted in 1980. These vessels have each operated at least 5,000 hours per year which translates to 15,000 hours of experience per vessel with cracked ligaments [1-6]. In none of these instances have the cracks been known to propagate more than 1 $^{1}/_{2}$ inches below the block top surface. Furthermore, the engines are still in service and are considered by the user to be fully operational.

1.2 Block and Liner Configuration

In general the dimensions of the block top are the same for the inline and V-engines based on a review of TDI engineering drawings [1-7 through 1-10]. Block top thickness, liner dimensions, cylinder head stud spacing, and the boss region below the block top which supports cylinder head studs are similar for all R-4 and RV-4 engine models.

The geometry of cylinder block, cylinder liner, cylinder head, and cylinder head studs is shown in cross section in Figure 1-11. The cylinder head nuts clamp the head onto the liner, which is supported by the liner landing ledge in the block. Two gaskets are located between the head and the cylinder block and liner. The gaskets are crushed and conform to the depth of the gasket grooves, based on measurements of gaskets removed from service. A typical plan view of a block top is shown in Figure 1-12, and block top sections are shown in Figures 1-13 and 1-14. Dimensions of the liner are shown in Figure 1-15.

The cylinder liner collar protrudes above the cylinder block top surface after installation by an amount which is called liner "proudness". TDI has stated that the specified liner proudness has been reduced in two steps from 5 to 9 mils to 3 to 5 mils and subsequently to the currently specified value of 0 to 3 mils [1-11]. A review of engineering drawings provided for SNPS engines indicates a liner proudness of 4 to 6 mils; the average measured value is 5 mils. The effect of reducing liner proudness is to reduce the portion of the cylinder head stud clamping preload that is carried vertically through the liner collar onto the liner landing ledge. The remaining portion of the clamping load is distributed over the top of the cylinder block by the cylinder head.

1.3 Material Specifications

The TDI R-4 series cylinder blocks are specified to be manufactured from gray cast iron in accordance with ASTM A48-64 Class 40, as required by TDI Drawing 03-315-03-AC. Specified minimum physical properties of the block material are also listed in Table 1-5.

The fatigue endurance limit of gray cast iron is related to the tensile strength. For Class 40 gray cast iron, the lower bound tensile strength is 40 ksi and the estimated endurance limit is 17.5 ksi [1-12]. However, the expected minimum tensile strength of gray cast iron is a function of the section thickness. For a 2 $^1/_2$-inch thick section, the minimum tensile strength of Class 40 gray cast iron is reduced to 32 ksi and the endurance limit to 14 ksi.

A typical S-N curve for Class 50 gray cast iron is shown in Figure 1-16. The S-N curve of Class 40 gray cast iron, is expected to be similar, as sketched in Figure 1-16, but with a lower endurance limit. The knee of the curve for Class 40 gray cast iron is not expected to shift much. Further data regarding fatigue of cast iron was identified in SEE conference papers [1-13 and 1-14]. These data produced the lowest curve on Figure 1-16. Though not specifically identified as experimental data from Class 40 gray cast iron, the tensile strength presented with the data does agree with Class 40 specifications. More specific Class 40 S-N data were not found in a review of the literature.

Section 1 References

1-1 "Evaluation of the Operational and Maintenance History of, and Recent Modifications to, the Main Engines in the M.V. Columbia," Seaworthy Engine Systems, Report No 123-01, April 1983.

1-2 Telephone conversation, R. Taylor, FaAA, with Dave Stallsberg, Mississippi Power and Light on 6/13/84.

1-3 Telephone conversation of 6/7/84 between M. Spiegel, FaAA, and Mr. Bruce Liberty, Senior Engineer, United States Steel, Great Lakes Fleet.

1-4 Telephone conversation, G. King, FaAA with Jim Fillingame, Copper Valley Electrical Association on 6/6/84.

1-5 Telephone conversation, G. King, FaAA with John Smith, Director of Generation, City of Homestead 6/6/84.

1-6 Telephone conversation, G. King, FaAA with Bob Grindland, Biehl Offshore, Inc. on 6/6/84.

1-7 TDI Block Drawing Nos. 03-315-03-AC, and 02-315-03-AE.

1-8 TDI Liner Drawing Nos. 03-315-02-0E, and 02-315-02-0G.

1-9 TDI Stud Drawing No. 03-315-01-0A.

1-10 TDI Cylinder Head Drawing No. 03-360-03-0F.

1-11 TDI Letter May 4, 1984 to Stone & Webster Engineering.

1-12 C. F. Walton and T. J. Opar, "Iron Castings Handbook," Iron Castings Society, Inc., 1981.

1-13 J. W. Fash, D. F. Socie, E.S. Russell, "Fatigue Crack Initiation and Growth in Gray Cast Iron," Materials, Experimental and Design in Fatigue, Proc. of Fatigue 1981, Society of Environmental Engineers (SEE) Conference, March 1981.

1-14 C. E. Bates, "Effect and Neutralization of Trace Elements in Gray and Ductile Iron," Ph.D Thesis, Case Western Reserve University (1968).

TABLE 1-1

ENGINE 101 LOAD HISTORY
SHOREHAM NUCLEAR POWER STATION

Event and Date	Hours at Load, L (%)					Total Hours, All Loads
	L<75	75<L<100	L=100	100<L<110	L>110	
Original Crankshaft Hours	164.0	262.5	188.5	--	19.0	634
Crankshaft replaced Restart 12/29/83 Testing Hours	78.0	179.0	20.0	91.0	4.5	372.5
Outage 3/18/84 Block Inspection 3/20/84 Qual. Testing Hours 4/10/84	43.0	10.0	29.5	.5	2.0	85
Total	285.0	451.5	238.0	91.5	25.5	1091.5

TABLE 1-2

ENGINE 102 LOAD HISTORY
SHOREHAM NUCLEAR POWER STATION

Event and Date	Hours at Load, L (%)					Total Hours, All Loads
	L<75	75<L<100	L=100	100<L<110	L>110	
Original Crankshaft Hours	83.0	325.0	259.0	22.0	--	689
Crankshaft Replaced Restart 12-22-83 Testing Hours	34.5	183.0	36.5	70.0	--	324
Outage 2/09/84 Block Inspection 2/10/84 Qual. Testing Hours	90.0	3.5	16.0	0.5	--	110
Block Inspection 3/08/84						
Total Hours	207.5	511.5	311.5	92.5	--	1123

TABLE 1-3

ENGINE 103 LOAD HISTORY
SHOREHAM NUCLEAR POWER STATION

Event and Date	Hours at Load, L (%)					Total Hours, All Loads
	L<75	75<L<100	L=100	100<L<110	L>110	
Original Crankshaft Hours	103.0	432.0	257.0	---	23.0	815
Crankshaft Replaced Restart 12/17/83 Testing Hours	67.0	170.5	69.0	34.5	6.0	347
Outage 3/11/84 Block Inspection 3/11/84 Qual. Testing Hours	54.5	5.5	24.5	13.0	1.0	108.5
Block Failure 4/14/84 Block Inspection 4/16/84 Total Hours	234.5	608.0	350.5	47.5	30.0	1270.5

TABLE 1-4

CATAWBA 1a ENGINE LOAD HISTORY

	Load, L (%)				
	L Unknown	L<82	82<L<100	L>100	Total Hours, All Loads
Hours at Load	201	48	373	188	810

GRAND GULF ENGINE LOAD HISTORY

	Load, L (%)					
	L Unknown	L<60	60<L<100	L=100	L=110	Total Hours, All Loads
Hours at Load	442	564	75	301	14	1396

TABLE 1-5

TYPICAL CYLINDER BLOCK MATERIAL PROPERTIES

Material	ASTM A48 - Class 40 (Minimum Property)
Tensile Modulus of Elasticity:	16×10^6 psi
Poisson's Ratio:	0.24
Ultimate Tensile Strength	40 ksi
Linear Coefficient of Thermal Expansion	6.6×10^{-6} in/in°F
Endurance Limit (Lower Bound):	17.5 ksi
Ultimate Tensile Strength (adjusted for 2.5-inch thick section):	32 ksi
Endurance Limit (Adjusted for 2.5-inch thick section):	14 ksi

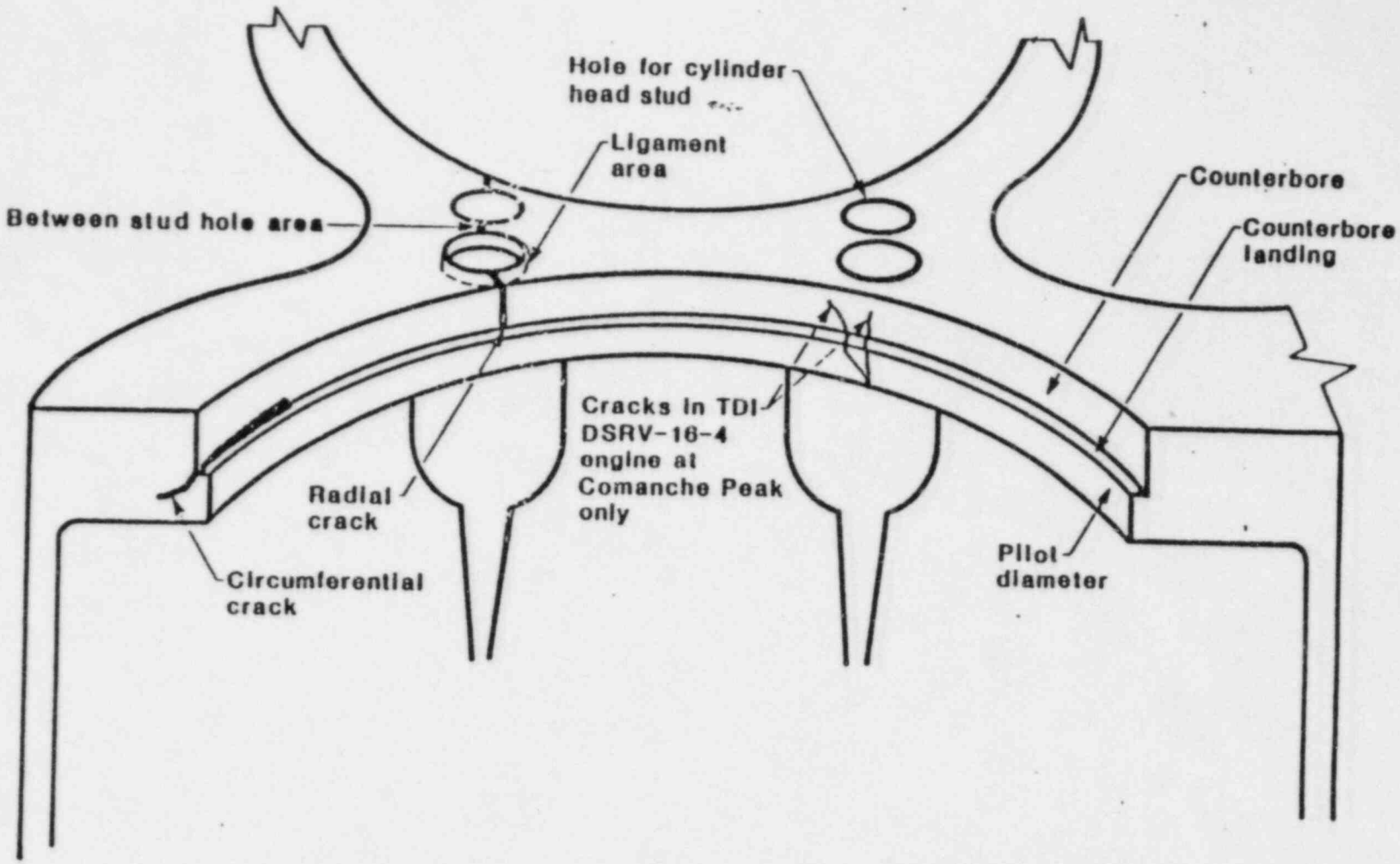

Figure 1-1. Location of cracks.

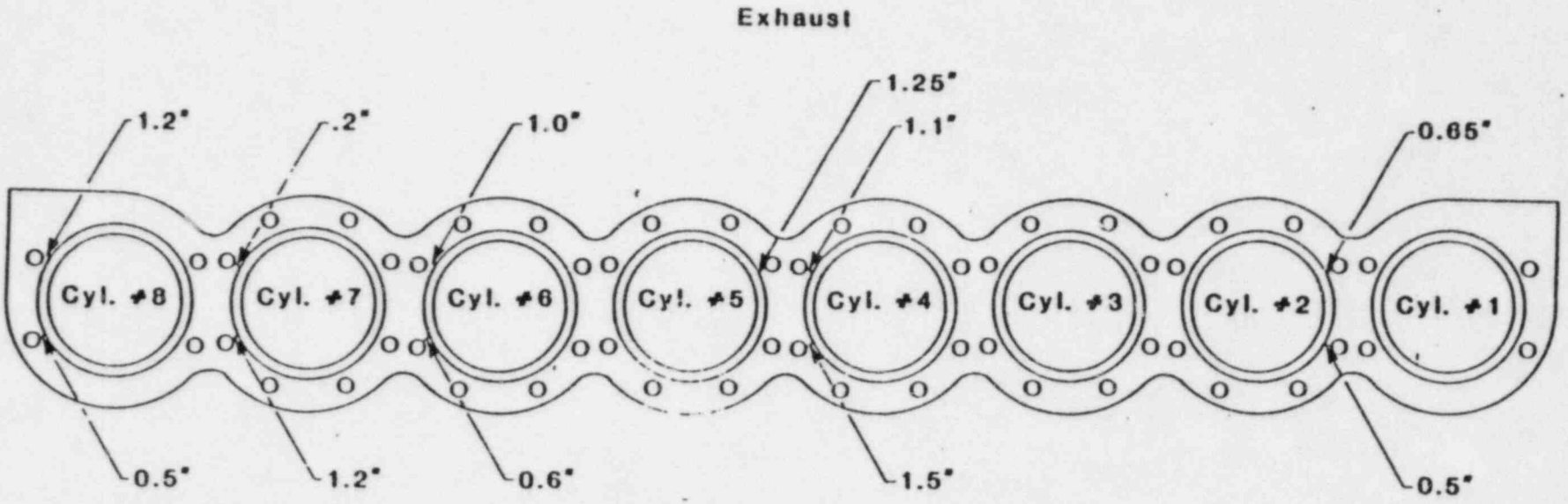

Figure 1-2. SNPS DG101 crack map.

FaAA-84-5-4

Ref: TER Q-308, TER Q-329, Q-95

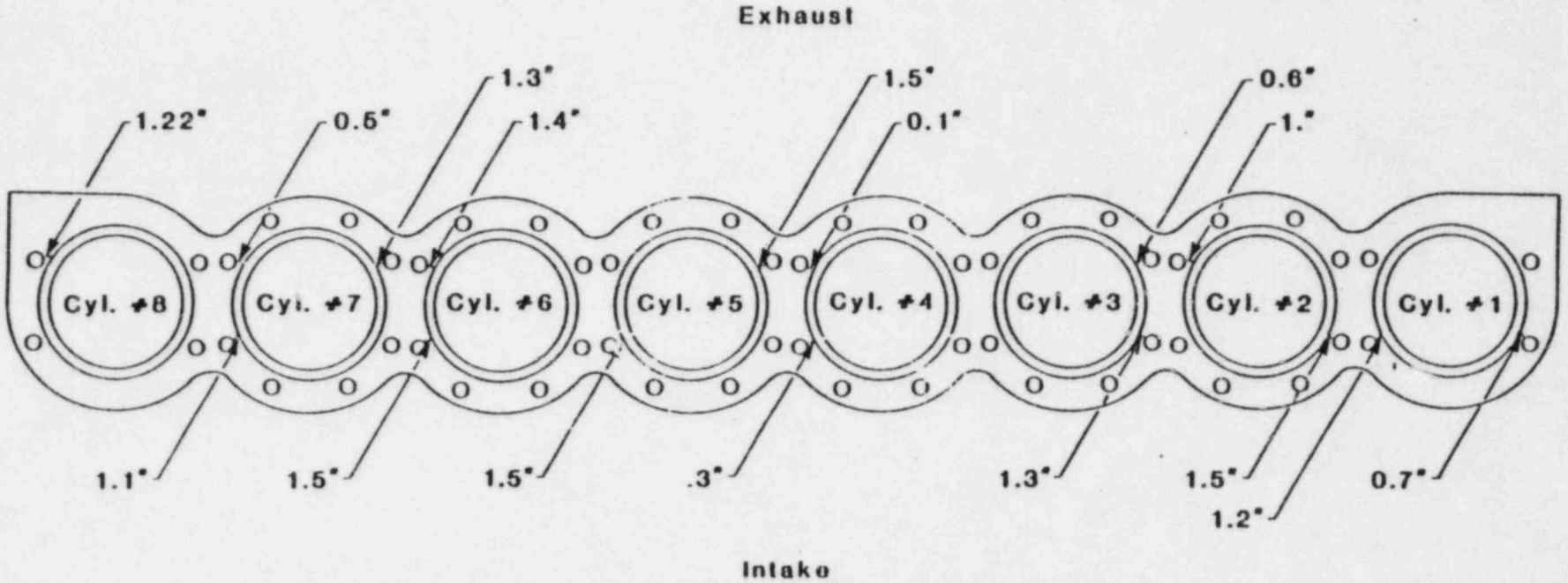

Dimensions indicate crack depth

Figure 1-3. SNPS DG102 crack map.

FaAA-84-5-4

Ref: LPDR-220

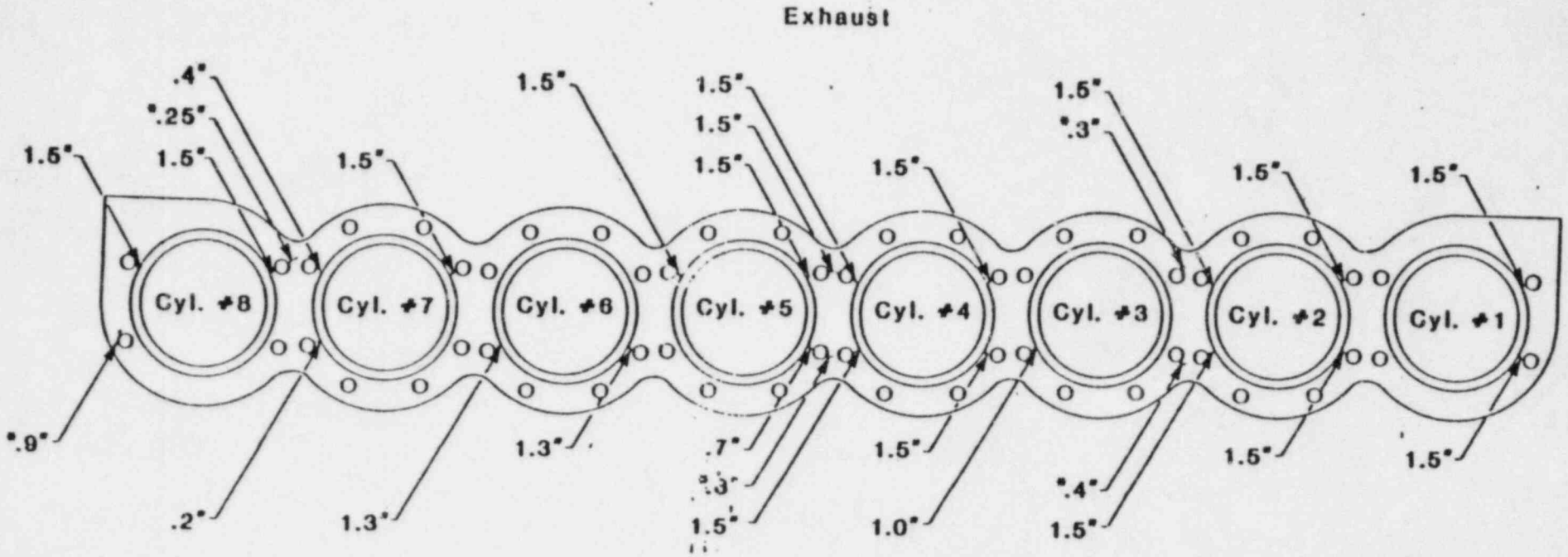

Dimensions indicate crack depth

*Top surface indication. Depth not measured

Figure 1-4. SNPS DG103 crack map as of 3/11/84.

FaAA-84-5-4

Ref: TER Q-130

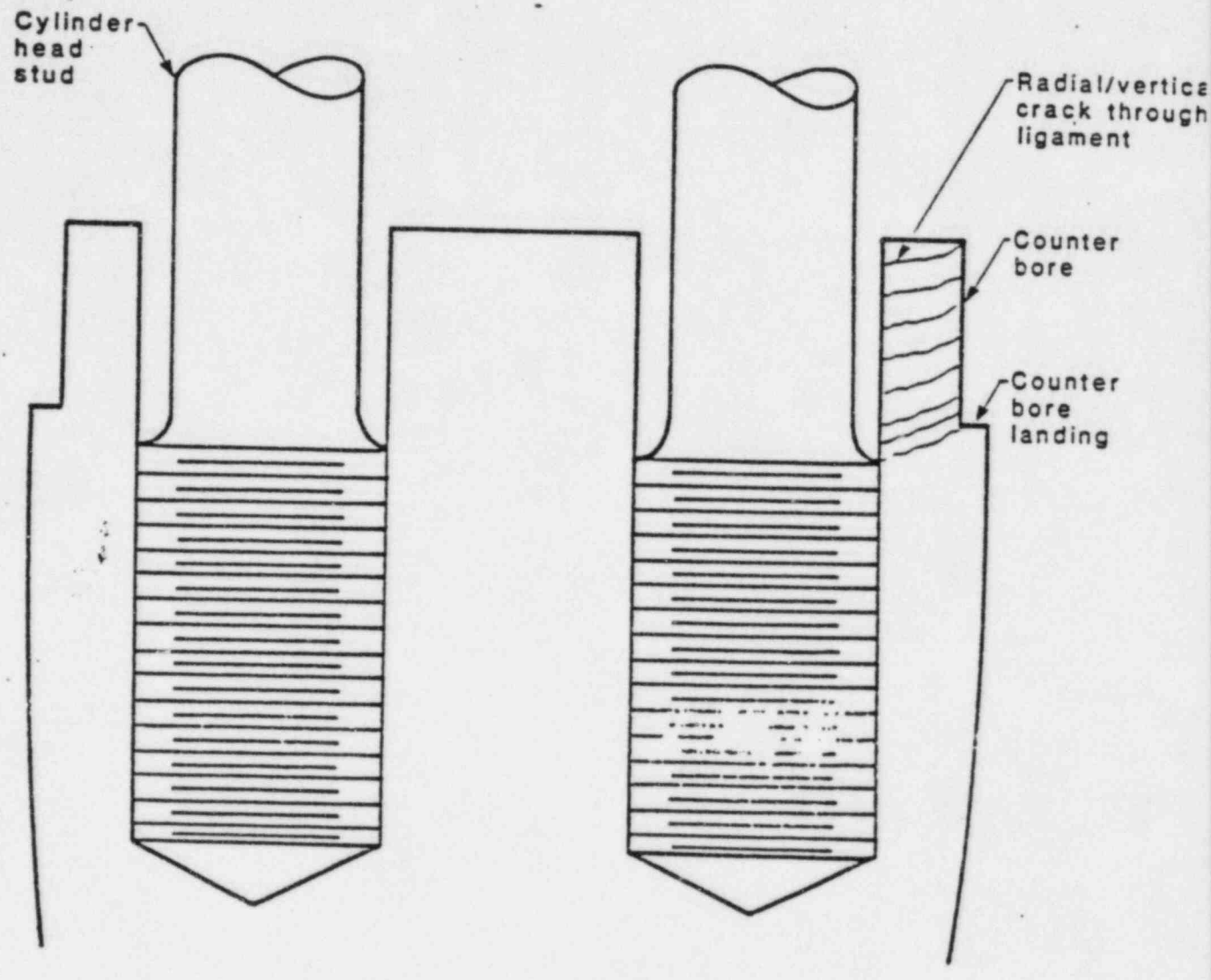

Figure 1-5. Longitudinal section between adjacent cylinders.

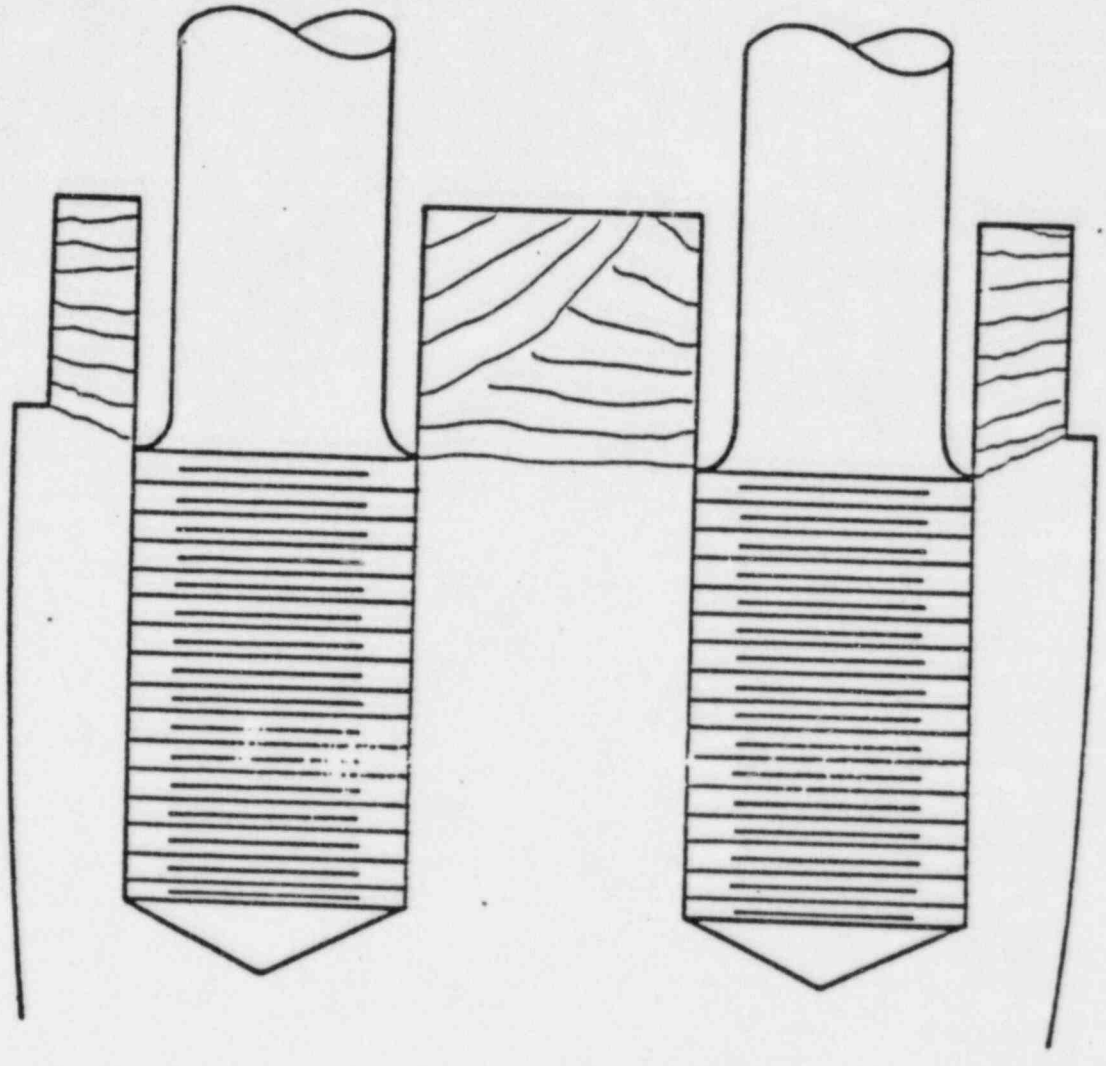

Figure 1-6. Longitudinal section between adjacent cylinders for SNPS DG103.

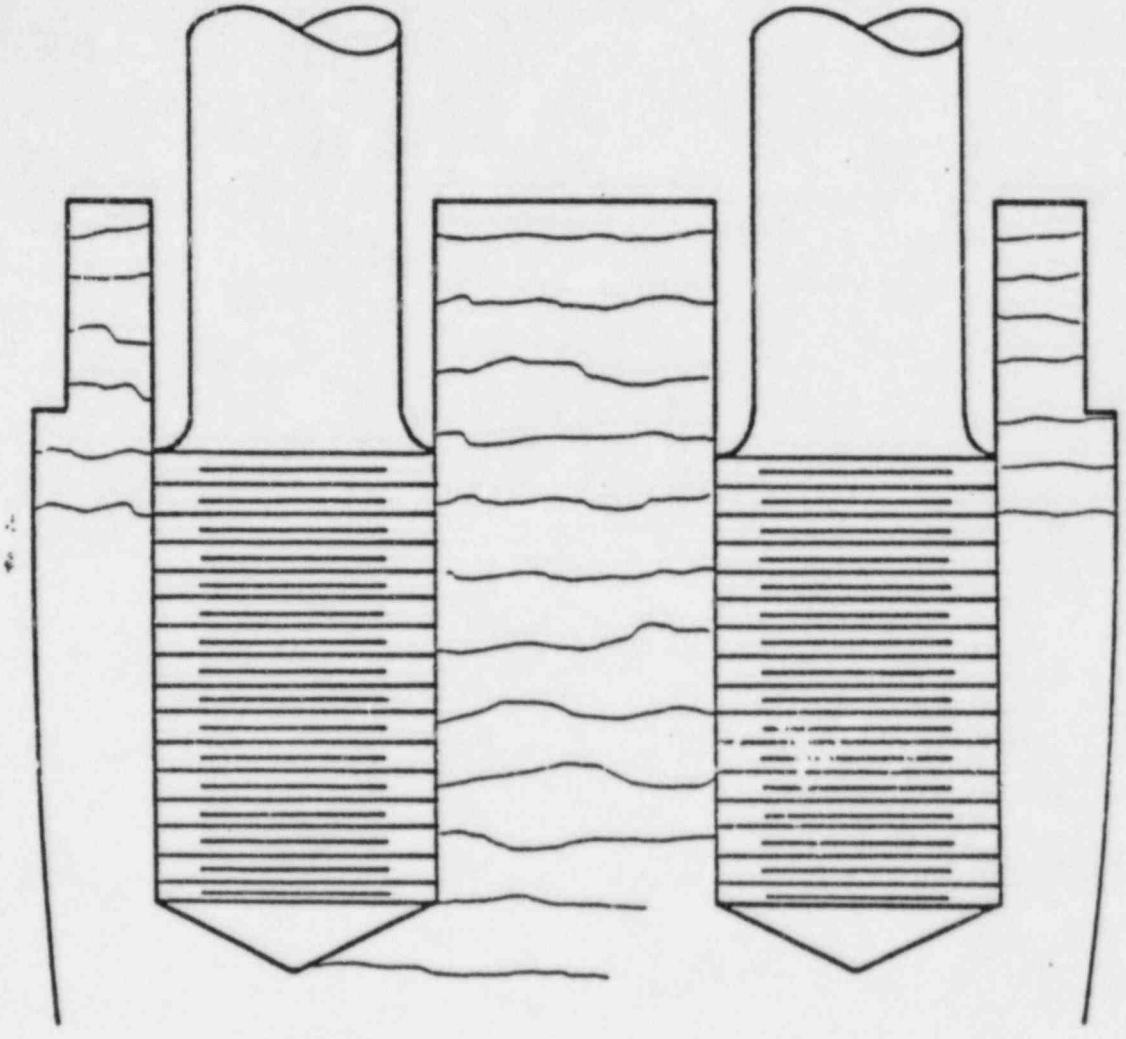

Figure 1-7. Longitudinal section between Cylinders 4 and 5 on exhaust side of SNPS DG103.

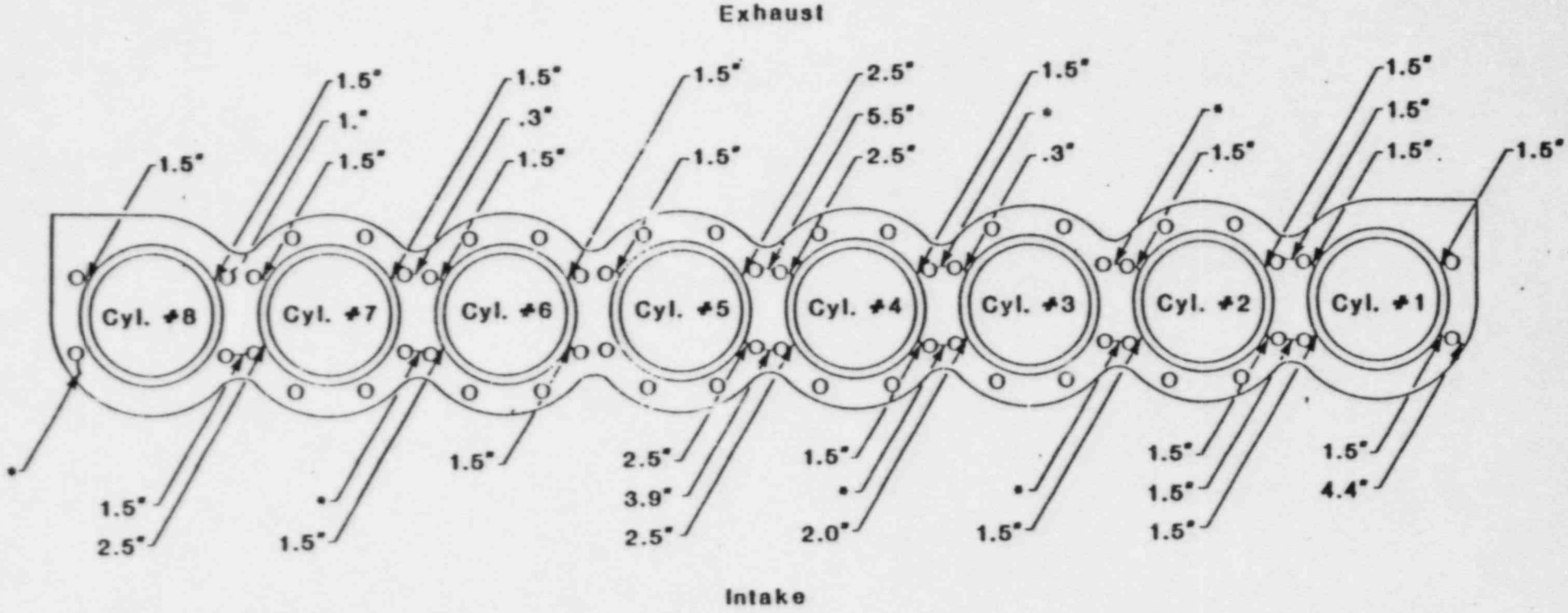

Dimensions indicate crack depth

*Top surface indication. No depth to crack measurable down stud hole

Figure 1-8. [illegible] DG103 crack map as of 4/23/84.

FAA-84-5-4

Ref: Q-465

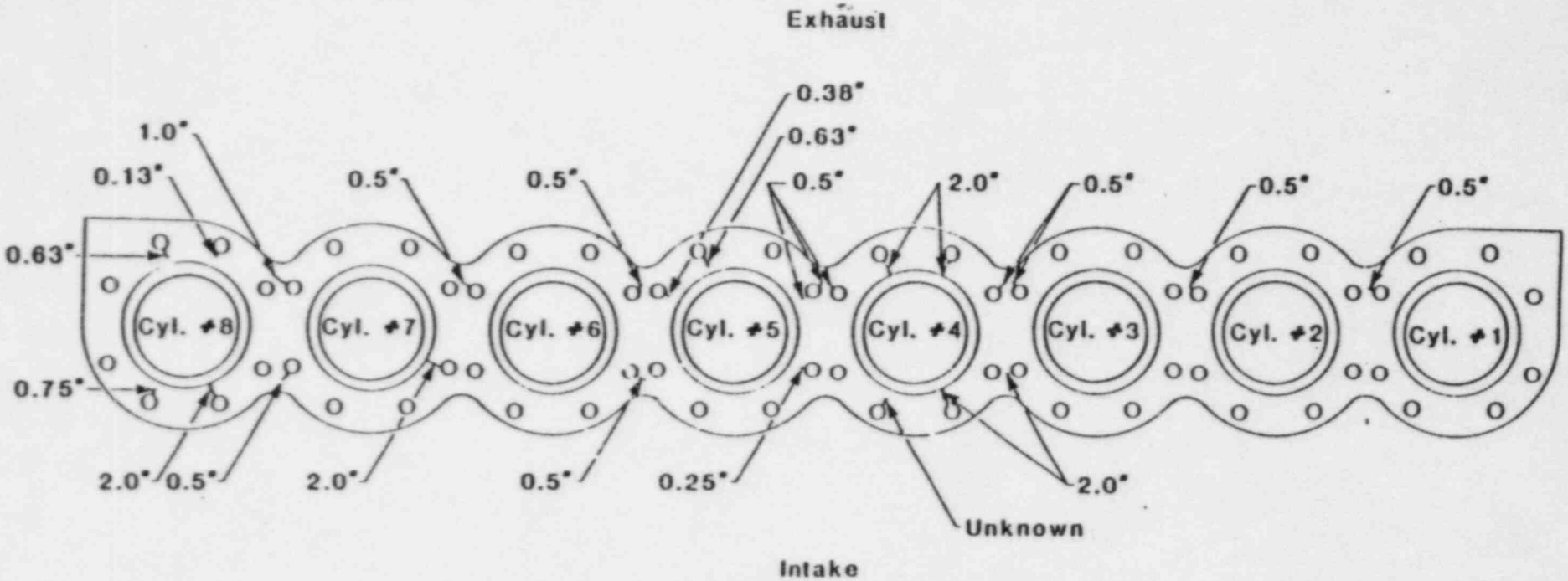

Figure 1-9. Engine crack map. Plan view of St. Cloud block top.

FAA-84-5-4

Ref: As reported by TDI

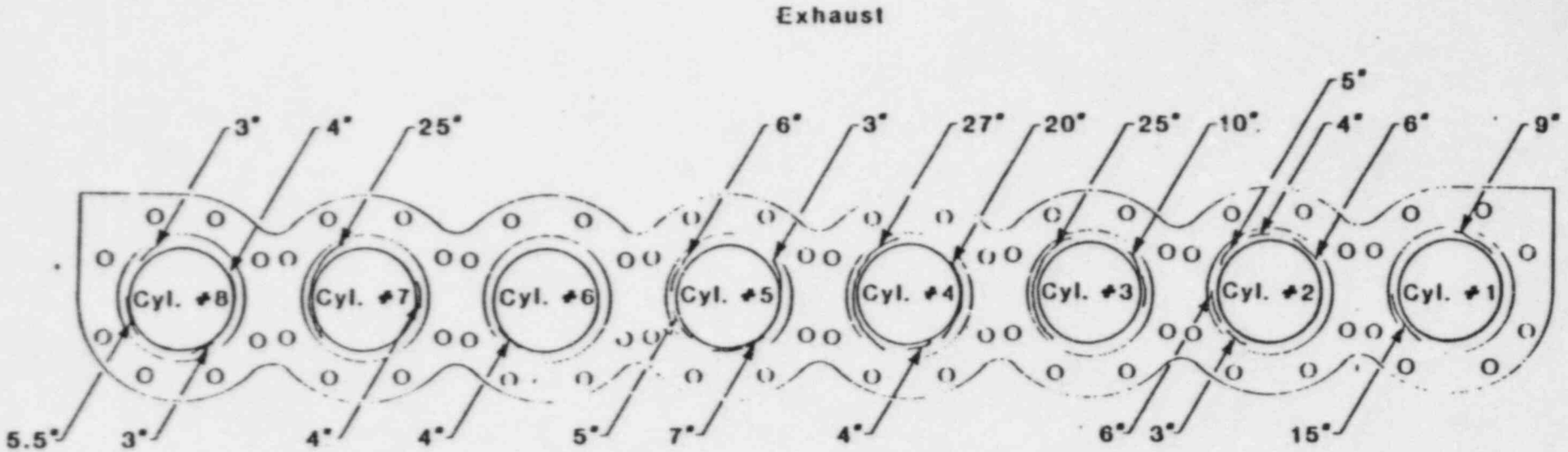

Figure 1-10. Engine crack map. Plan view of St. Cloud block top. Circumferential cracks in liner landing.

FAA-84-5-4

Ref: As reported by TDI

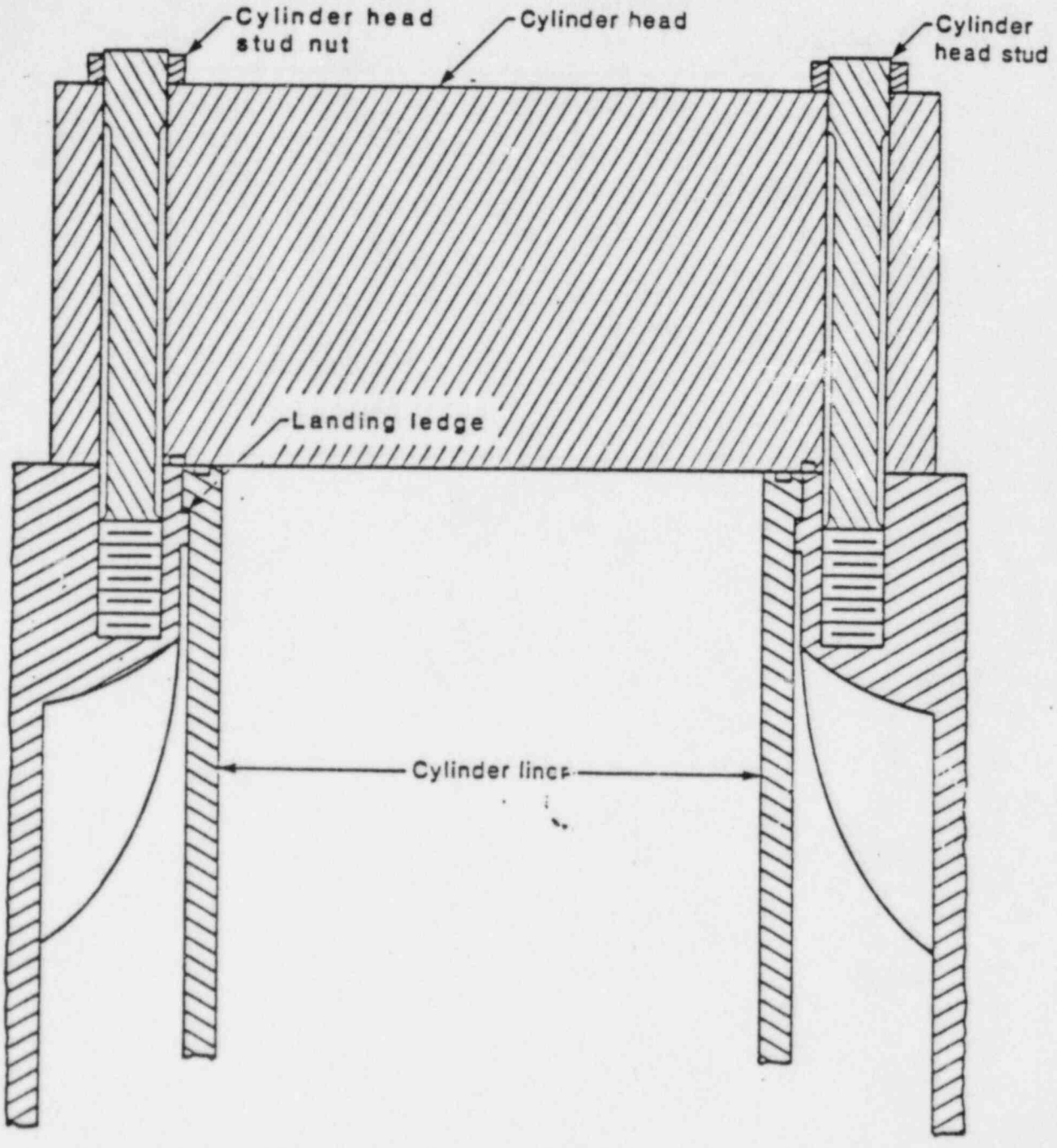

Figure 1-11. Typical configuration.

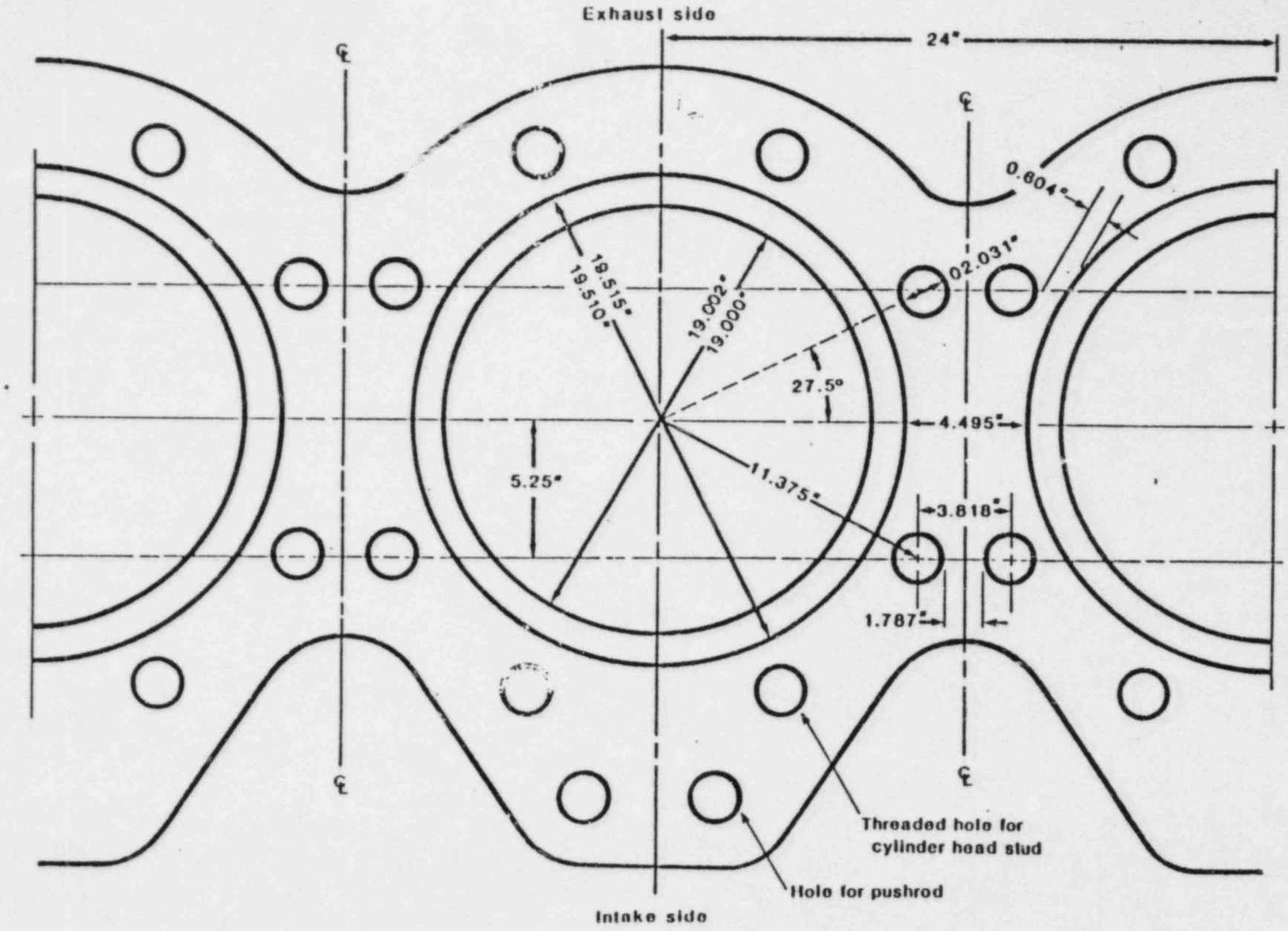

Figure 1-12. Block top dimensions. Reference block, TDI drawing no. 03-315-03-AC.

FAA-84-5-4

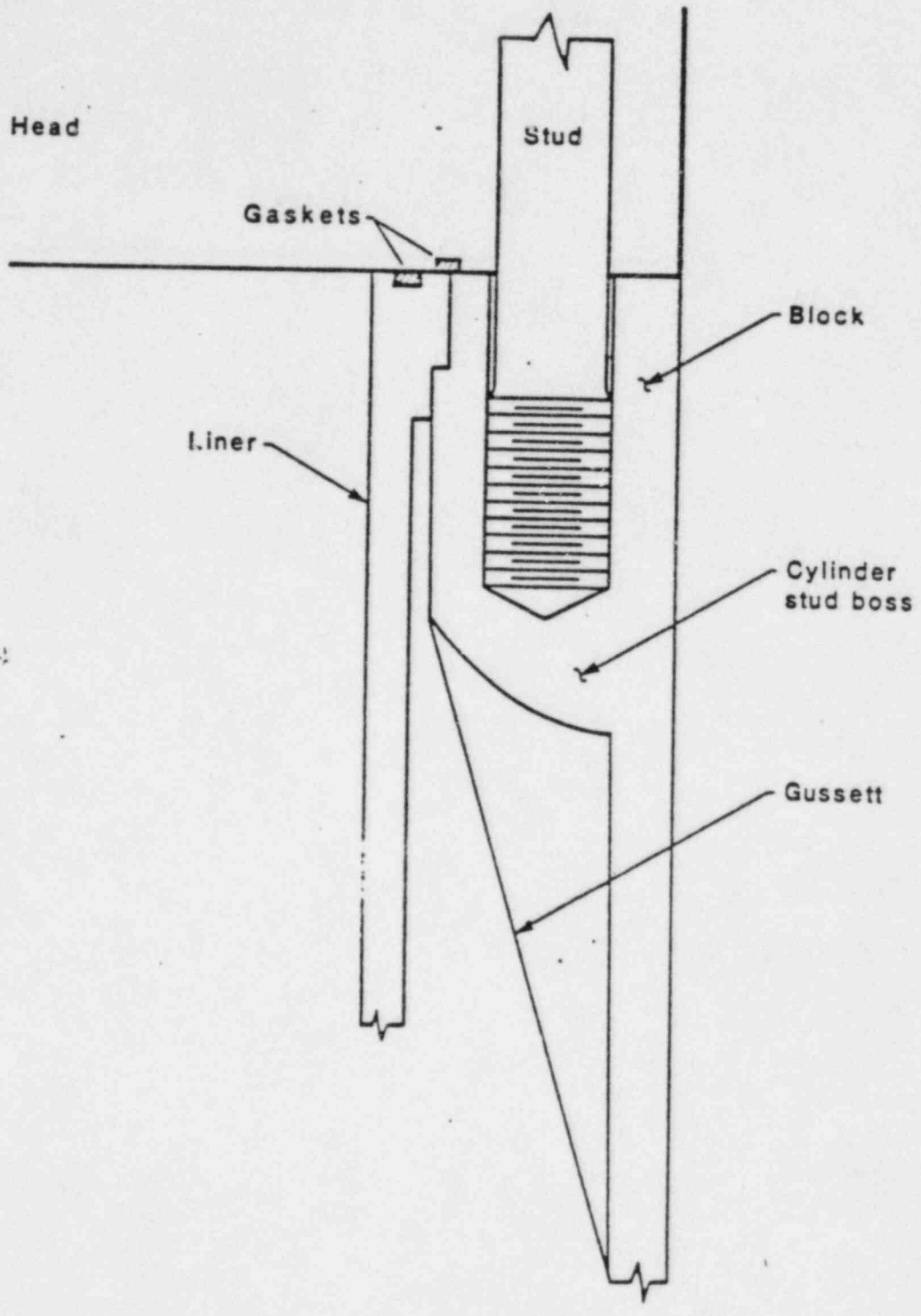

Figure 1-13. Section through cylinder head stud.

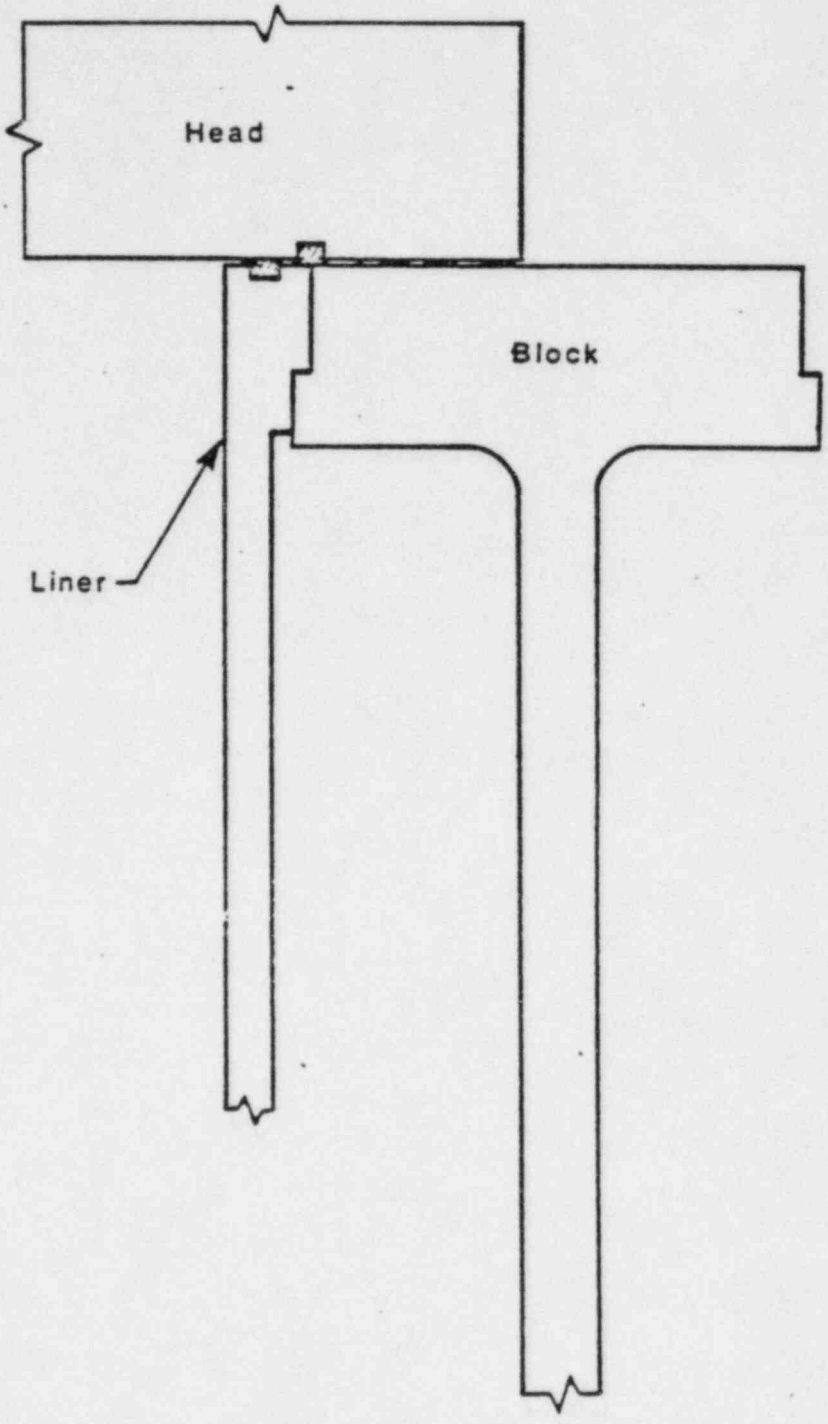

Figure 1-14. Section through non-stud region.

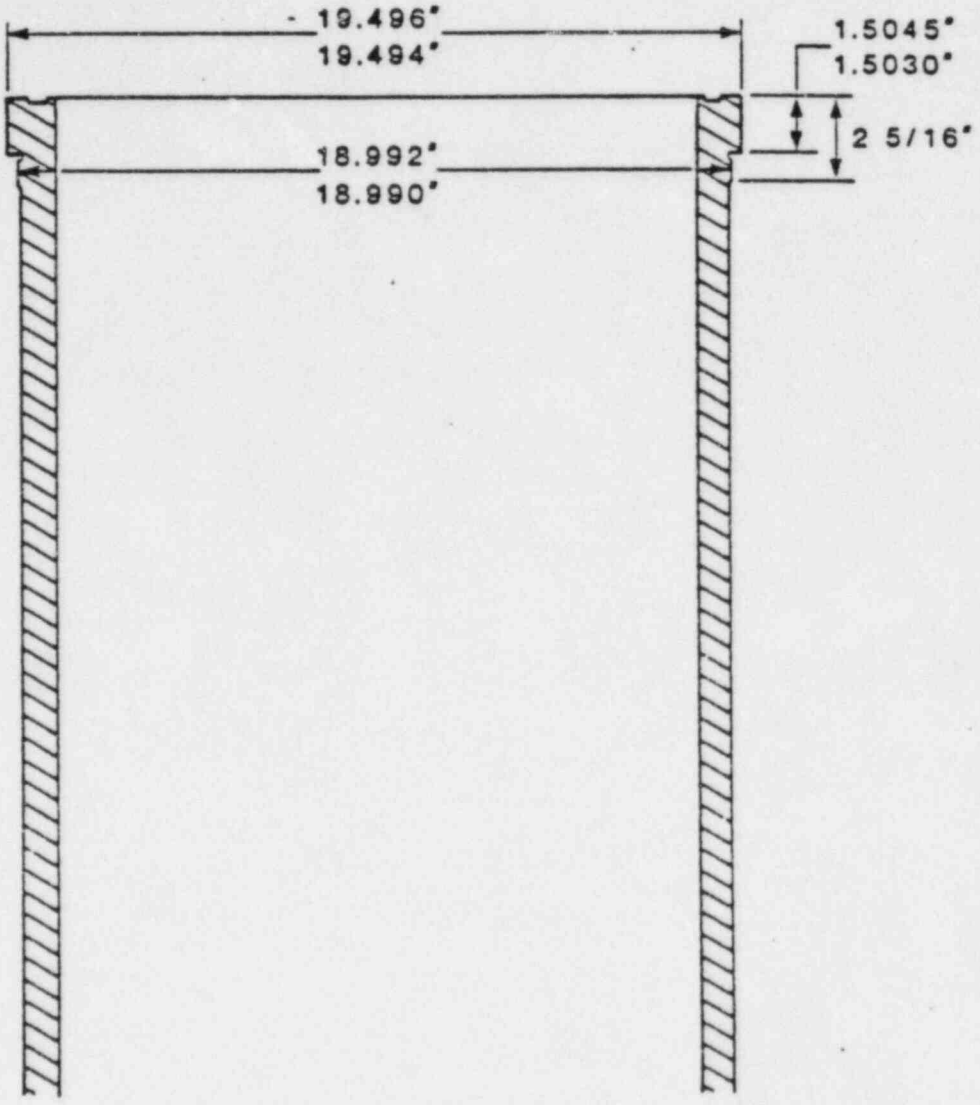

Figure 1-15. Cylinder liner.

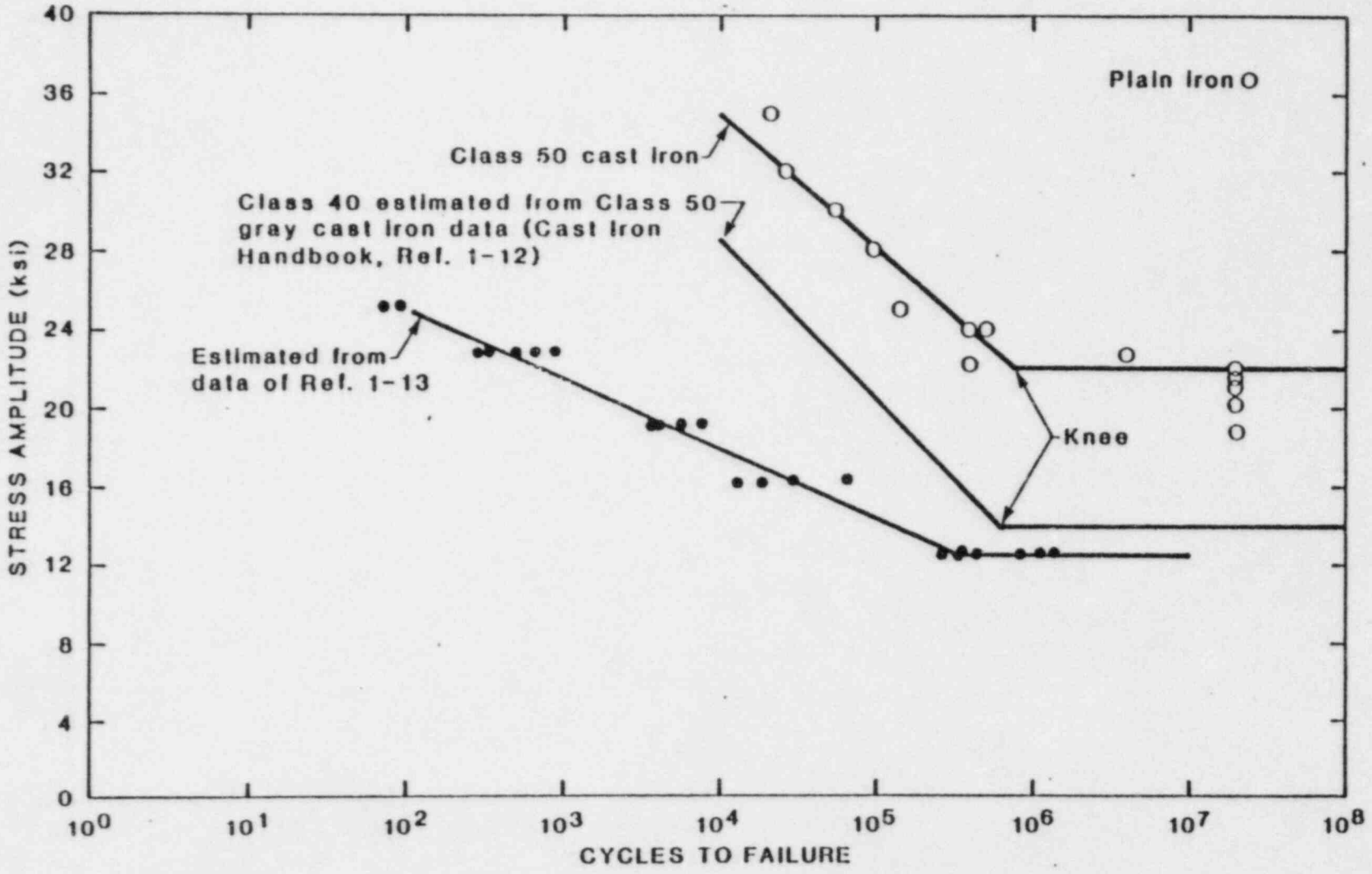

Figure 1-16. S-N curve for gray cast iron.

FAA-88-5-4

2.0 LOAD ANALYSIS

Loads on the block that potentially influence fatigue and fracture include the preload on the cylinder head studs, the load distribution between the cylinder head and the block, the load between the head and the liner collar, and the thermal and pressure loads between the liner and the block. These loads result in bending and in-plane stresses in the block top and shear stresses at locations of concentrated loads. The distribution of these loads and resulting stresses is affected by the distortion of the cylinder head, liner, and block top. Since the loading and distortion are interacting and very complex, strain gage measurements and several 2-D models have been analyzed to help deduce the most significant contributions to the block stress.

2.1 Preload

The primary loading on the block consists of the preloading of the cylinder head by the eight head studs, totaling about 1×10^6 lbs on each head [2-1 and 2-2]. Each firing stroke pushes the head upward against the preload with a force of 255* p_{max}, where p_{max} is the peak firing pressure in psi. This load is typically 400,000 lbs, or 40% of the stud preload. About 13% of the firing load adds to the stud preload (stud forces increase by 5%) while the remainder of the firing load reduces the clamping pressure between head and block.

Much of the preload is transmitted from the fire deck of the cylinder head to the top of the liner collar. The actual amount depends upon the bending stiffnesses of the fire deck and the block top, thermal distortion, and the vertical protrusion of the liner collar above the block top. The cylinder head also contacts the block, as shown by patterns in used block tops. The combination of stud preload and vertical liner collar reaction results in a couple tending to rotate the edge of the block downward and resulting in tensile stress directed radially towards the cylinder.

*The area bounded by the midline of the gas seal is approximately 255 square inches.

The stud preload also results in bending moments about radial lines through the stud holes, producing circumferential bending stresses in the block top that are tensile at the stud holes and compressive midway between adjacent stud holes for the same cylinder. The magnitude of this bending stress is governed by the deflection of the cylinder head and block top, which depends on the amount of preload, radial clearances, and the protrusion of the liner above the block top.

The studs have 2-8N-2A threads [2-3]. Consequently, there is a "bursting pressure" or radial component outward from the stud arising from the 30° pressure angle of the thread (relative to the horizontal plane). This radial component causes a hoop stress in the vicinity of the top threads, 1.78 to 3 inches below the top of the block.

The combined effect of the preload is radial and circumferential bending plus vertical and radial thread loads, a complex 3-D stress state. Both the block and head distort to accommodate the bending.

2.2 Thermal Loads

The liner and block top have a thermal gradient from the cylinder bore to the centerline between adjacent cylinders, such that $T_A > T_B > T_B^1 > T_C$ in Figure 2-1. The liner and block both expand radially from the cylinder centerline as the temperatures rise, creating thermal stresses. Because of the thermal gradient, the liner expands more than the block, closing the liner-to-block clearance gap and adding interference stresses. The combined effect is a radial stress in the block top that is resisted by circumferential tension. The effect of the stud holes is to make the stresses non-uniform in the circumferential direction, with circumferential tension near the stud holes and compression midway between adjacent stud holes for the same cylinder.

Thermal loads are also caused in and carried through the cylinder heads. As the fire deck heats up, it expands radially, and this motion is transmitted to the block through the friction between head and liner or block. In addition, the studs may be pushed radially outward from the center of the block, adding concentrated moments in the threaded region.

Depending on the clearance, some or all of the radial expansion stresses of the liner will be resisted by the liner hoop strength, rather than be transferred to the block. There is an optimum clearance which fully utilizes the available clearance gap so that the liner is in continuous contact with the block, but the interference stresses in the block are as small as possible. Some of the head expansion stresses may also be resisted by the liner hoop strength, if the friction force between head and liner is greater than that between head and block (due to liner proudness).

2.3 Pressure Loads

Radial forces due to cylinder firing pressure produce alternating hoop stress in the cylinder liner. The peak firing pressure for the SNPS R-4 engines is approximately 1600 psi. Assuming that the thermal loads have closed the clearance gap between liner and block, the pressure inside the liner is resisted by the liner and block hoop strength. The resistance is not uniform around the circumference, however, because the ligament at each stud hole is relatively flexible and can bend away from the liner. At those locations, the liner resists relatively more of the firing pressure, the block relatively less. Between studs, the liner and block have similar stiffness, so they share the pressure load as one continuous member.

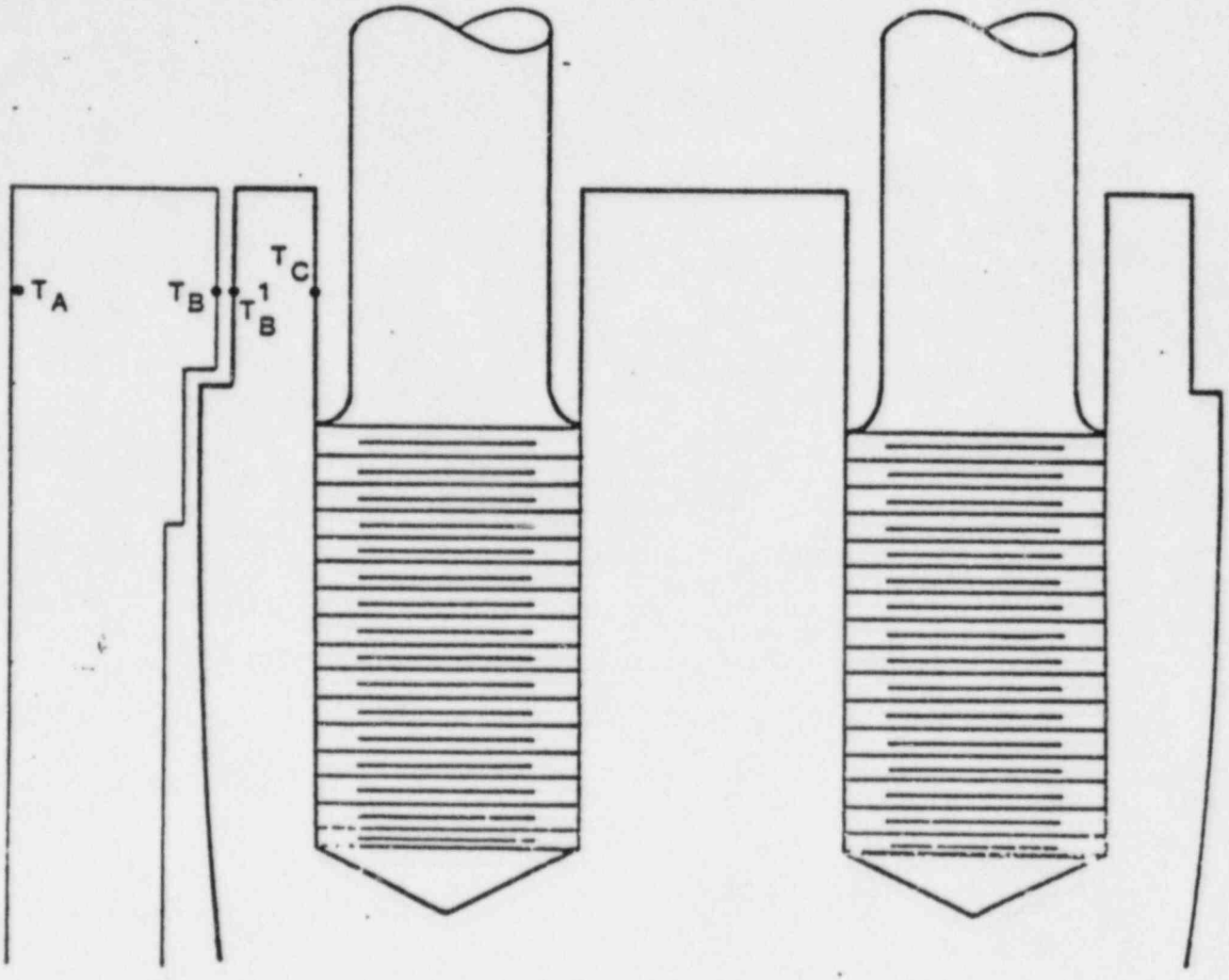

Figure 2-1. Location of T_A, T_B, T_B^1, T_C.

3.0 STRESS ANALYSIS

Sufficient analysis and testing have been completed to qualitatively understand the load components in the cylinder block and to provide estimates of the stress levels caused by these contributors (i.e., stud preloads, cylinder firing pressure, temperatures, and assembly clearances). The analysis is focused on two locations of observed cracking, the ligament between a stud hole and a liner counterbore and the region between studs of adjacent cylinders. Table 3-1 summarizes source of data or analysis and Table 3-2 gives the numerical results for stud preload, and thermal and pressure loads at these locations. The results are given for 90%, 100%, and 110% of full load rating.

3.1 Strain Gage Testing

This subsection presents the results of strain gage tests on SNPS DG103. Complete test data results are contained in a supplementary report [3-1]. Excerpts of the data are repeated here for clarity. Additional data are included from strain gage tests conducted by TDI [3-2] with different gage locations.

After the 100 hour full power endurance test run on SNPS DG103, a cylinder block strain gage test was conducted by FaAA. The test included strain measurements at three locations: midway between Cylinder Nos. and C, on the centerline between the adjacent exhaust side cylinder head studs; between Cylinder Nos. 5 and 6 at the intersection of the longitudinal and transverse centerlines between the cylinders; and at Cylinder No. 1 between the No. 3 cylinder stud and the edge of the engine. The location and nomenclature for the three gages are shown on Figures 3-1 and 3-2.

Measurements of strain versus preload were made while the cylinder head stud nuts were being tightened. The eight studs for each cylinder were tightened in three load increments: 1200, 2400, and 3600 ft-lbs torque.

Strain measurements during steady operation were recorded at 0, 873, 1500, 2000, 2500, 3500 (full load), and 3830 kW. To verify strains during thermal transients, measurements were recorded during slow starts, a quick

start to full load, and a LOOP/LOCA simulation. No strain measurements during thermal transients were in excess of the peak steady-state values. Therefore, the quick start requirement for nuclear emergency diesel generators does not place more severe loads on the block top than are experienced in non-nuclear service without quick starts.

Figures 3-3 and 3-4 depict the strain components for each gage during preload and operation. The band of data at operational loads depicts the range of the signal from each gage in the rosette for Gage Nos. 8 through 13. The arrows represent the direction of the strain during firing. This data was reduced to principal stresses as shown in Figures 3-5 and 3-6 for Gage Nos. 8 through 13. The maximum principal stresses were approximately parallel to Gage Nos. 8 and 13. The key stresses for stud-to-stud crack initiation and propagation are those measured by Gage No. 13.

TDI also conducted strain gage testing of preload and operating stresses in the liner and liner counterbore regions [3-2]. Selected results are given in Table 3-2 for their Gage Nos. 3 and 4, which were reading hoop strains in the locations shown in Figure 3-7. These gages measure key stresses for ligament cracking.

Note from the TDI Gage No. 4 in Table 3-2 that preload and pressure stresses do not decrease rapidly with depth: preload stress is still near 10 ksi at 2 inches below the block top, and the firing pressure range is 3 ksi. This suggests that the apparent arrest of ligament cracks at about 1 $^{1}/_{2}$-inch depth, evident in the inspection results, may be due to a displacement limit on the crack opening, rather than to a favorable stress gradient. This is consistent with the theory that ligament cracks of any depth are fully contained between the intact liner and the region of the block top outside the stud hole circle. Once the load initially carried by the cracked ligament region is redistributed to liner and outer block top regions, there is no driving force for further crack growth.

3.2 Finite Element Analysis

3.2.1 Two-Dimensional Block Top Model Without Ligament Crack

A qualitative understanding of the effects of pressure, liner temperature, and assembly clearance on stresses at the stud hole counterbores has been obtained from a 2-D finite element model of a quarter section of the block top. The finite element model, shown Figure 3-8, represents the block top and liner between the engine centerline and the midplane between adjacent cylinders. The liner is assumed to have expanded due to thermal stresses such that the gap is closed. The inner boundary of the liner was subjected to uniform pressure loading, and the symmetrical boundaries were restrained against rotations and displacements normal to the boundaries. Two sets of boundary conditions were analyzed, symmetric (both adjacent cylinders have internal pressure) and antisymmetric (one has pressure, the other zero pressure). Both thermal and pressure effects could be analyzed by combinations of these two cases. The model neglected the 3-D effects of the web between the cylinders and the cylinder head stud bosses beneath the block deck. Forces and deflections out of the plane of the block top were not included in this analysis.

This model was used directly to analyze the stresses in the ligament resulting from firing pressure in one cylinder, given appropriate clearances such that the liner-to-block gap is closed by thermal expansion. The results are shown in Figure 3-9 and Table 3-2. Reasonably good agreement with the pressure stress at full load at TDI Gage No. 4 is apparent in Table 3-2. The experimental pressure stress at Location 1 was scaled up from TDI Gage No. 4 using the stresses at the corresponding locations, i.e., 6.3 ksi = 3.3 (9.5/5), and the result is in reasonable agreement with the analysis at full load.

The model was also used to obtain the ratio of stresses in the ligament resulting from thermal expansion, using symmetric boundary conditions as in Figure 3-10. The thermal stresses are symmetric between cylinders because both cylinders heat up, analogous to both cylinders firing at once. All thermal stresses are assumed to act radially in the plane of the block top.

Under this assumption, Figure 3-10 can be used to scale the thermal stress from the Gage No. 13 reading to the ligament Location 1. However, Gage No. 13 corresponds to a cracked ligament, so it is necessary to scale the reading to reflect an uncracked ligament. For this computation the thermal stress is taken to be σ_{min} minus $\sigma_{preload}$. The result is 14.9 ksi = 9.7 (9.31/6.06) at 100% load.

The third application of the model was to determine the radial stress distribution on the inside surface of the block resulting from a uniform pressure on the inside surface of the liner. This distribution is not uniform around the circumference, as shown by Figure 3-11, where the distribution is superimposed on the cracked ligament model discussed below. The ligament will not support as much radial stress as the surrounding regions; rather, it bends away from the liner, which must therefore carry higher stress locally.

The fourth application was to determine the effect of varying the liner-to-block radial clearance. Assuming that the clearance is small enough so that the gap remains closed at temperature, an increase in clearance of 0.001 inch will reduce thermal ligament hoop stress at Location 1 by 2 ksi and thermal hoop stress at Location 2 by 1 ksi. Table 3-2 was developed corresponding to about 0.005 inch radial clearance near the block top.

3.2.2 Two-Dimensional Block Top Model With Ligament Crack

Once a ligament crack is present, the transverse stress between the stud holes increases by a factor of 2. This is shown (for pressure stresses) by the model shown in Figure 3-11, where the radial stress distribution was determined from the stress at the liner/block interface in the uncracked model. The results are shown in Table 3-2 and Figure 3-12, which may be compared with Figure 3-9 at Location 2 and Gage No. 13. The stress at Location 2 is obtained by scaling the gage reading, i.e., 6.6 ksi = 3.7 (10.85/6.06) at 100% load.

The calculated pressure stress range is greater than the gage reading at each location. This is to be expected because the plane strain block top model assumes that there is a crack all the way through the ligament. In the

real case, the ligament crack is only about 1 $^1/_2$ inches deep, so less stress is actually transferred to the stud-to-stud region than is calculated by the model.

As in Section 3.2.2, the thermal stress is obtained by scaling the stress measured at Gage No. 13, using the model in Figure 3-11 to obtain the scaling factor. The primary assumption in this process is that the thermal stress acts in the plane of the block top, analogous to pressure. The result is 17.3 ksi = 9.7 (10.85/6.06) for 100% load.

3.3 Discussion of Stress State at Crack Sites 1 (Ligament) and 2 (Stud-to-Stud)

The stress shown in Table 3-2 can be divided into mean and alternating components for fatigue analysis. For low cycle fatigue caused by startup plus load change from 0% to a particular load level, the relevant alternating stress range is the peak stress at that load level (upper pressure band) minus the preload. This range may not be substantially different for starts from hot standby or cold starts, because the stress difference between cold preload and the lower pressure band for steady state running at zero load is less than 1 ksi, as shown by Gage No. 13 in Figure 3-6. The mean stress is the preload plus half of the range, while the alternating stress is half the range. For high frequency fatigue caused by the firing pressures, the relevant alternating stress range is that caused by firing (the band on each curve from the strain gages). The mean stress is the preload plus the thermal range plus the difference between average (mean) stress at load and the median stress in the stress band from firing. The alternating stress is half the range.

The results are shown in modified Goodman (Smith) diagrams: Figure 3-13 for ligament cracking and Figure 3-14 for stud-to-stud cracking given cracked ligaments. The curves are derived from the minimum ultimate tensile strength in thick sections, the minimum specified endurance limit (>10^6 cycles), and the stress for failure in 100 cycles (from the lowest curve in Figure 1-16). In both cracking locations, the stress state is outside the Goodman (Smith) curve for either HFF or LCF and for any load level of 90% or higher. The implication is that initiation of ligament cracks in minimum strength material

is predicted, and given a ligament crack, initiation of stud-to-stud cracks is also predicted. Initiation could occur in less than 100 load excursions from 0 to 90% power or above and/or steady running for more than 10^6 cycles (about 100 hours) at 90% power or above if the minimum material properties are assumed. At 110% load, overload failure could occur in both locations with minimum strength material since the peak total stress is 33 ksi compared to 32 ksi minimum thick-section ultimate strength. The fact that few blocks that have run at 110% load have cracks at both locations is indicative of higher-than-minimum material properties and/or conservatism in the analysis.

The stress components in Table 3-2 are believed to be best available estimates from strain gage readings or conservative analytic scaling to key locations from gage readings, except for the preload. The preload gage readings (Gage Nos. 3 and 13) were used directly without scaling, even though the stress due to preload is probably higher near the stud hole in Crack Locations 1 and 2. This unconservative preload estimate partly compensates for conservative adjustments to the thermal stresses and for the conservatism inherent in the analysis of cracked ligaments with a plane strain model. This analysis is also conservative for engines that operate at lower temperatures and/or pressures.

Other than determining the scaling factors to get from gage locations to crack initiation sites, the analytical models were used only for insight. Reasonably good agreement between all available experimental and analytical results was obtained for several 2-D finite element and hand calculation models. However, in such a complicated case, with interacting effects of clearance gaps, 3-D geometry and loading, friction, component-to-component distortion interactions, and relatively uncertain material properties, the experimental results are judged to be more reliable than the models.

Section 3 References

3-1 SNPS cylinder block DG103 strain gage test data FaAA Report 84-6-xx, in preparation.

3-2 TDI strain gage data, provided to FaAA by Greg Beshouri (TDI).

TABLE 3-1

METHOD OF DETERMINING STRESS ESTIMATES

Location		Stress Source			
				Pressure Range	
		Preload Experimental	Thermal Experimental	Experimental	Analytical
Ligament	TDI Gage No. 3	Gage reading	--	--	2-D plane model
	TDI Gage No. 4	Gage reading	--	Gage reading	2-D plane model
	Block top at stud hole Location 1	Use Gage No. 3 reading	Ratio from Gage No. 13 with 2-D plane model	Ratio from Gage No. 4 with 2-D plane model	2-D plane model
Between studs (for cracked ligament)	FaAA Gage No. 13	Gage reading	Gage reading	Gage reading	2-D cracked plane model
	Block top at stud hole Location 2	Use Gage No. 13 reading	Ratio from Gage No.13 with 2-D cracked plane model	Ratio from Gage No. 13 with 2-D cracked plane model	2-D cracked plane model

TABLE 3-2

CONSERVATIVE ESTIMATES OF STRESS NORMAL TO CRACK FACE AT CRITICAL LOCATIONS

Location		Stress (ksi)				
				Pressure Range		
		Preload Experimental	Thermal Experimental	Experimental	Analytical	Load Level %
	TDI Gage No. 3	8.2	--	--	5.0	100
Ligament	TDI Gage No. 4	10.5	--	3.1	--	90
		10.5		3.3	5.0	100
		10.5		3.6	--	110
	Block top at stud hole Location 1	8.2*	14.1	5.9	--	90
		8.2*	14.9	6.3	9.5	100
		8.2*	18.8	6.9	--	110
Between studs (for cracked ligament)	FaAA Gage No. 13	4.3	9.2	3.4	--	90
		4.3	9.7	3.7	6.06	100
		4.3	12.2	4.2	--	110
	Block top at stud holes Location 2	4.3*	16.4	6.1	--	90
		4.3*	17.3	6.6	10.85	100
		4.3*	21.8	7.5	--	110

*Unconservative

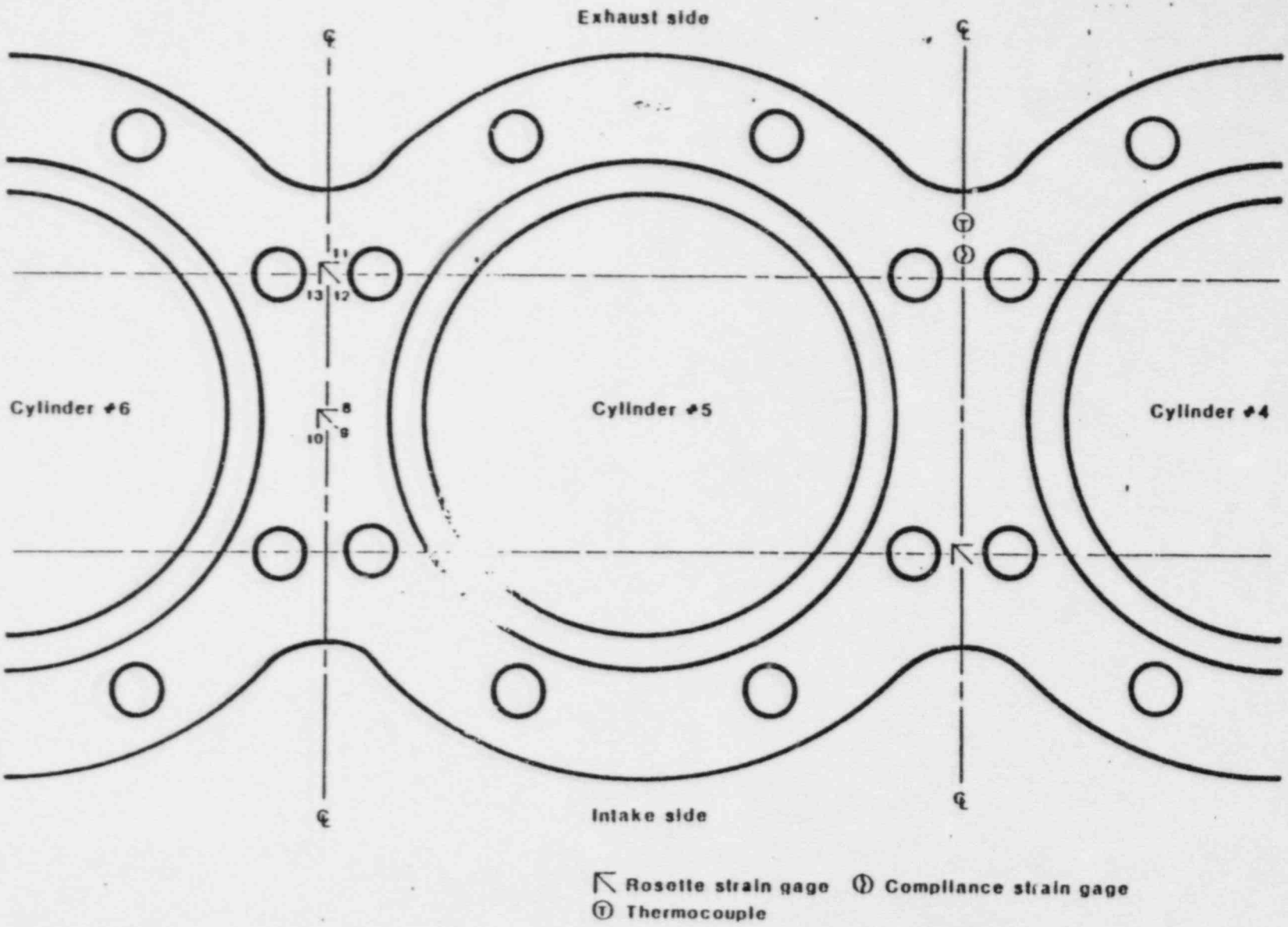

Figure 3-1. Strain gage placement.

FAA-84-5-4

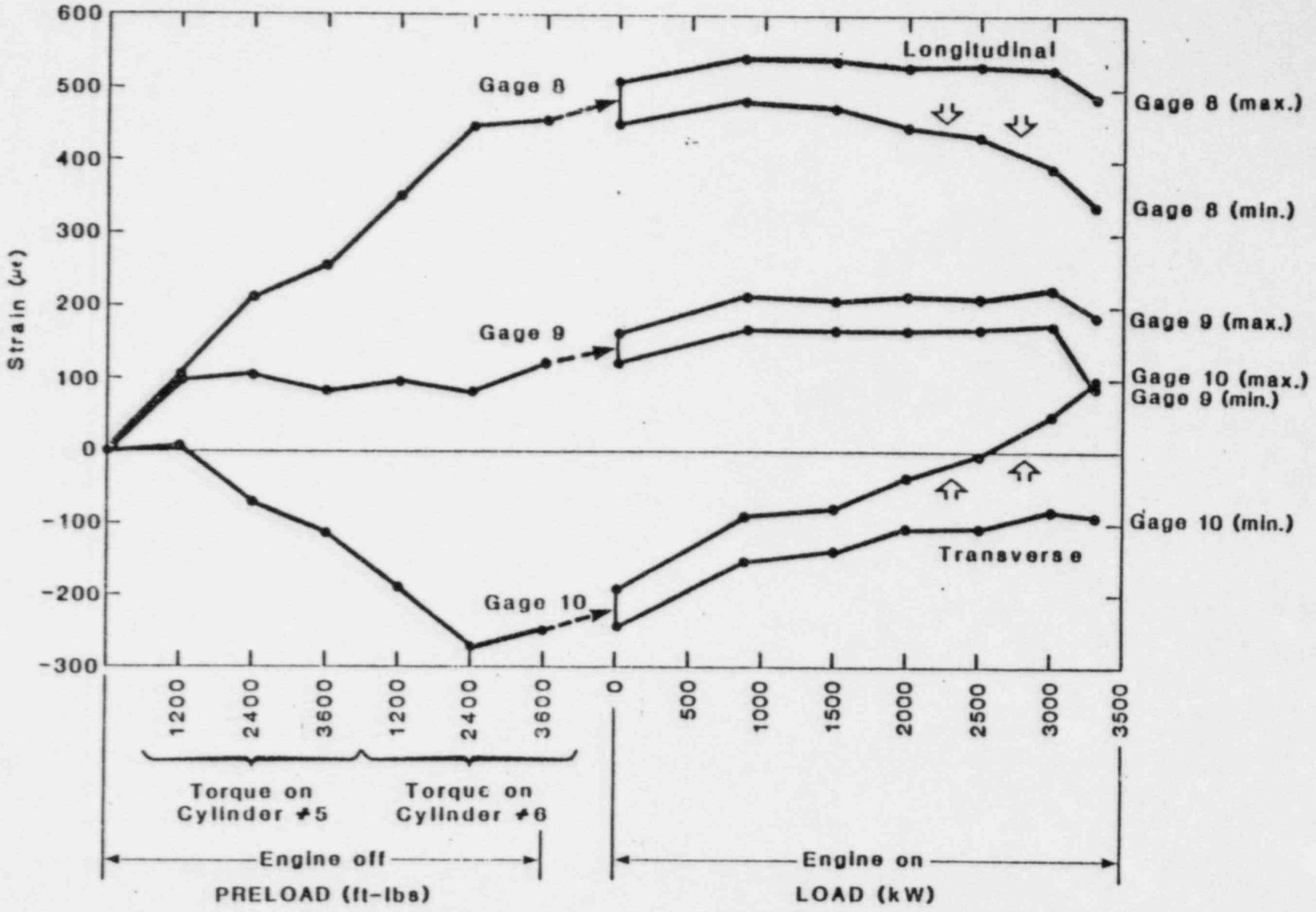

Figure 3-3. Strain vs. load for Gages 8, 9 and 10 (located on engine centerline).

FAA-84-5-4

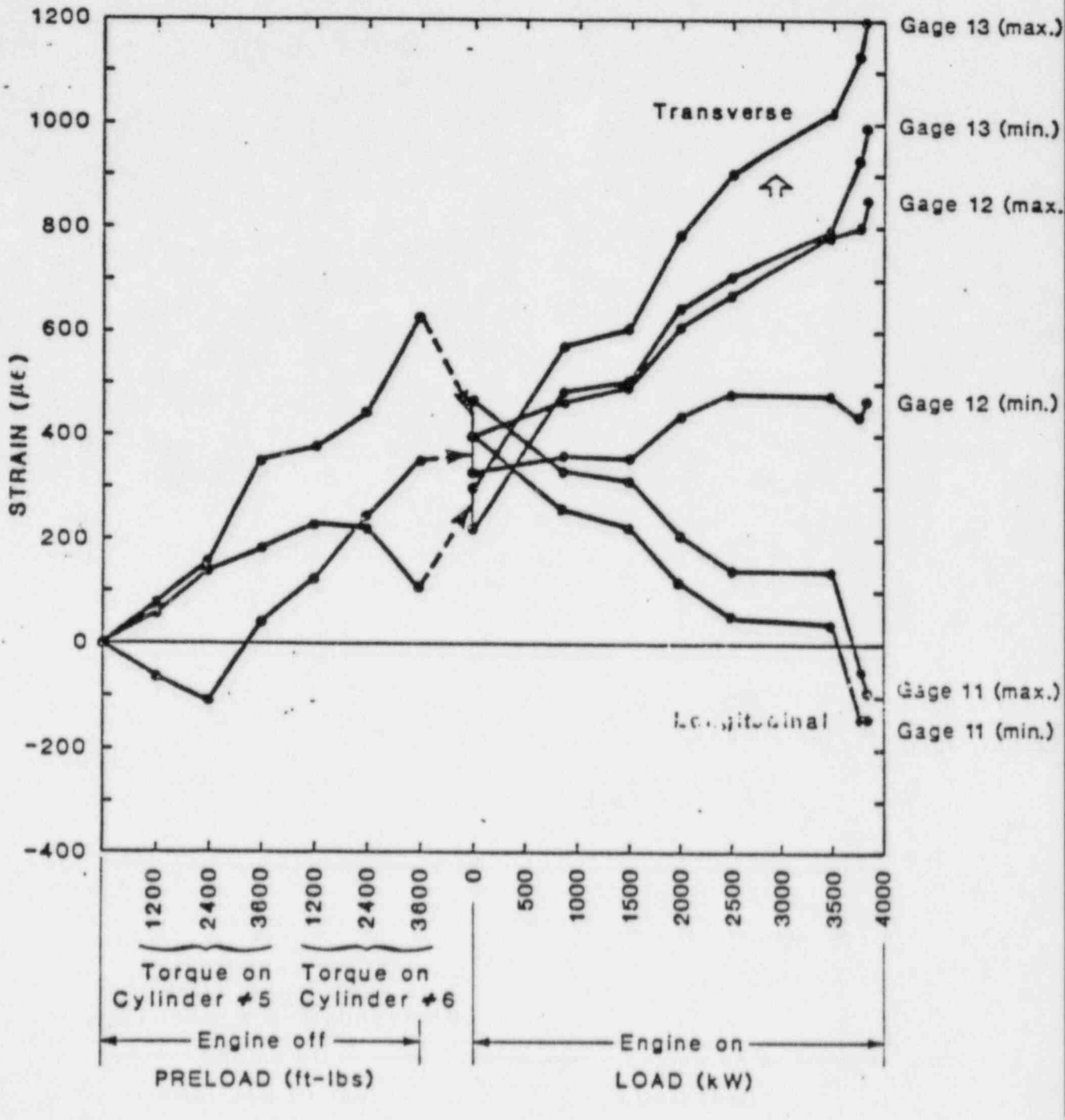

Figure 3-4. Strain vs. load for Gages 11, 12 and 13 (located between studs).

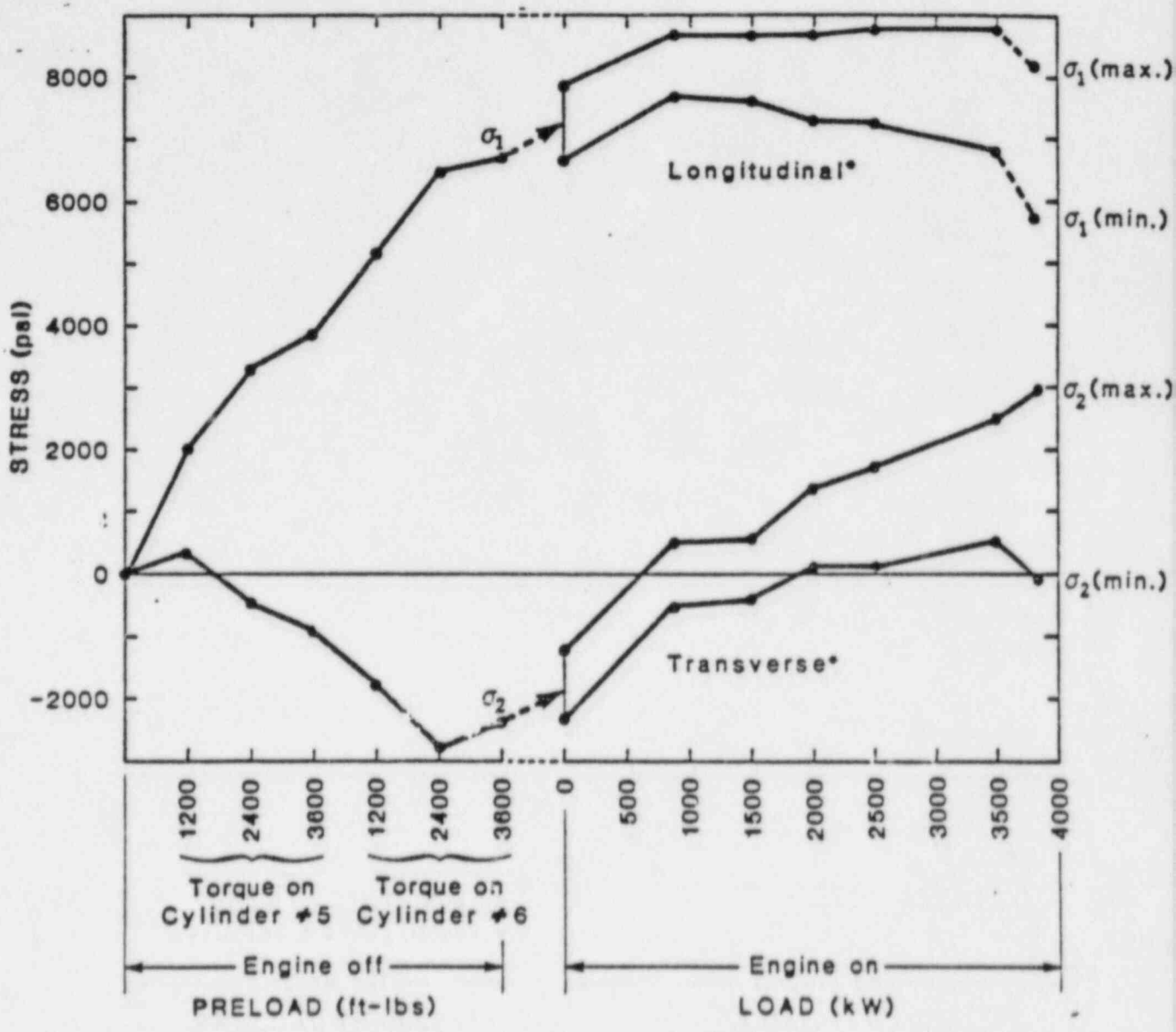

Figure 3-5. Principal stresses vs. load for Gages 8, 9 and 10 (located on engine centerline).
*Principal stresses are located within 12° of the transverse.

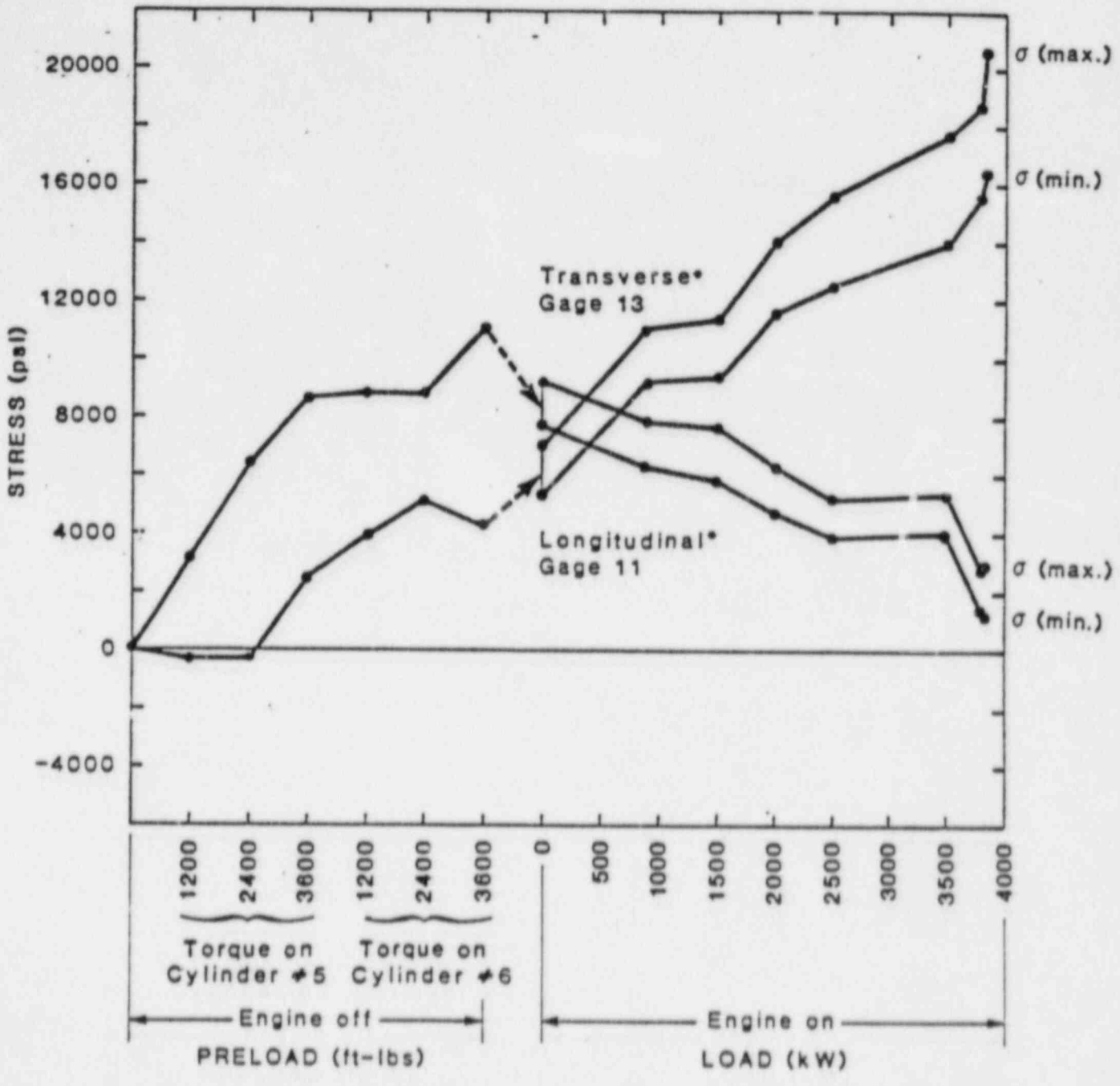

Figure 3-6. Principal stresses vs. load for Gages 11, 12 and 13 (located between studs.
*Principal stresses are located within 15° of gage axis.

FaAA-84-5-4

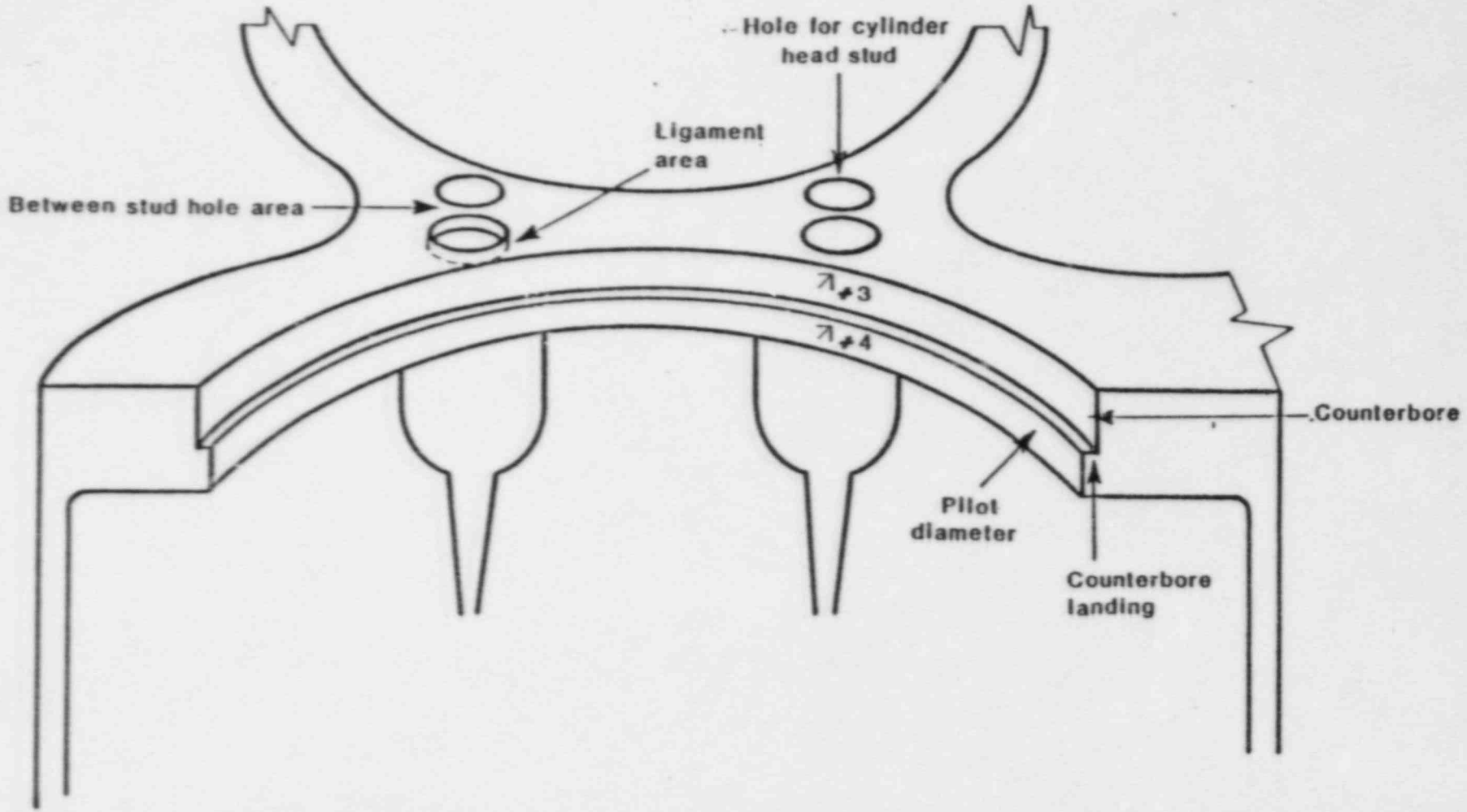

FAA-84-5-4

Figure 3-1. TDI strain gage location.

Ref. 3-1

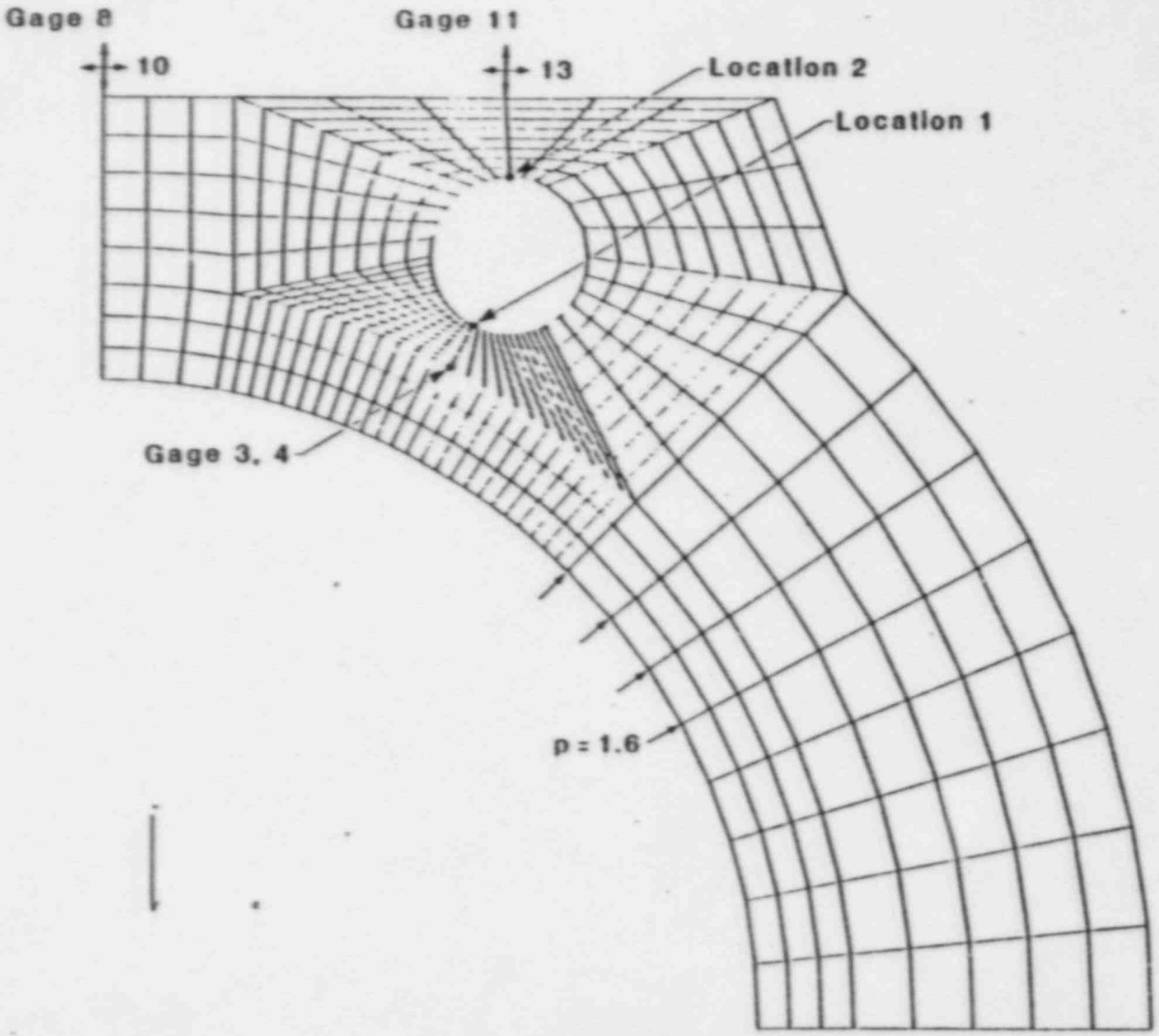

Figure 3-8. Block top model with internal pressure equal to 1.6 ksi.

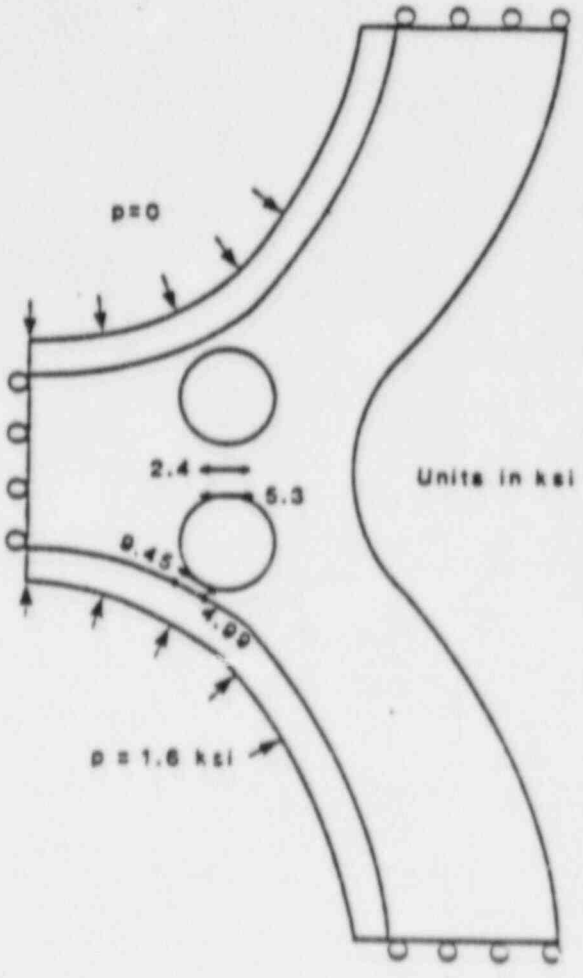

Figure 3-9. Effect of one cylinder firing.

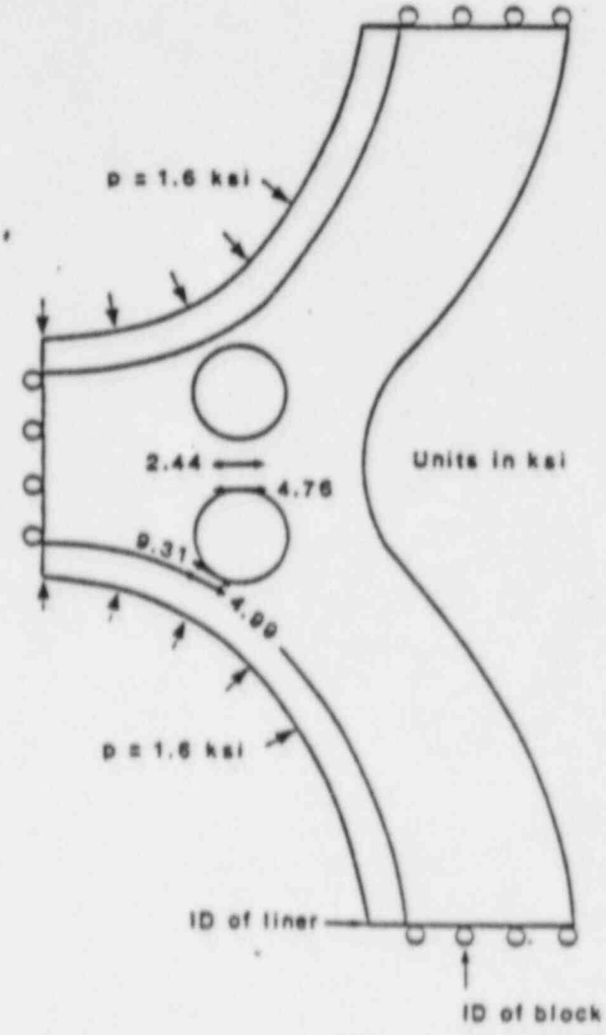

Figure 3-10. Block-top model (2-D) with liner subjected to internal pressure p = 1.6 ksi in adjacent cylinders.

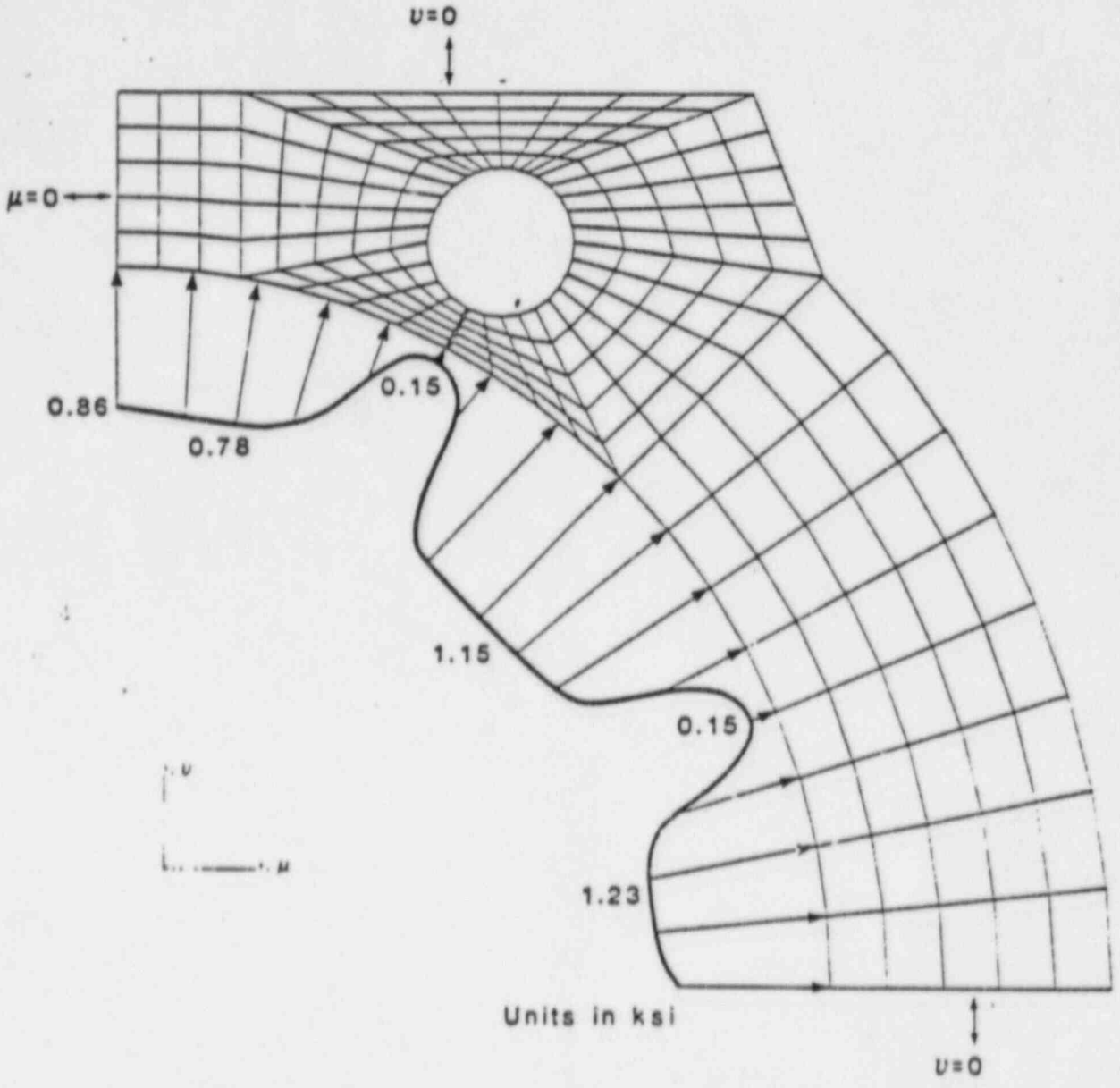

Figure 3-11. Cracked ligament block model with radial stress distribution due to liner under uniform pressure.

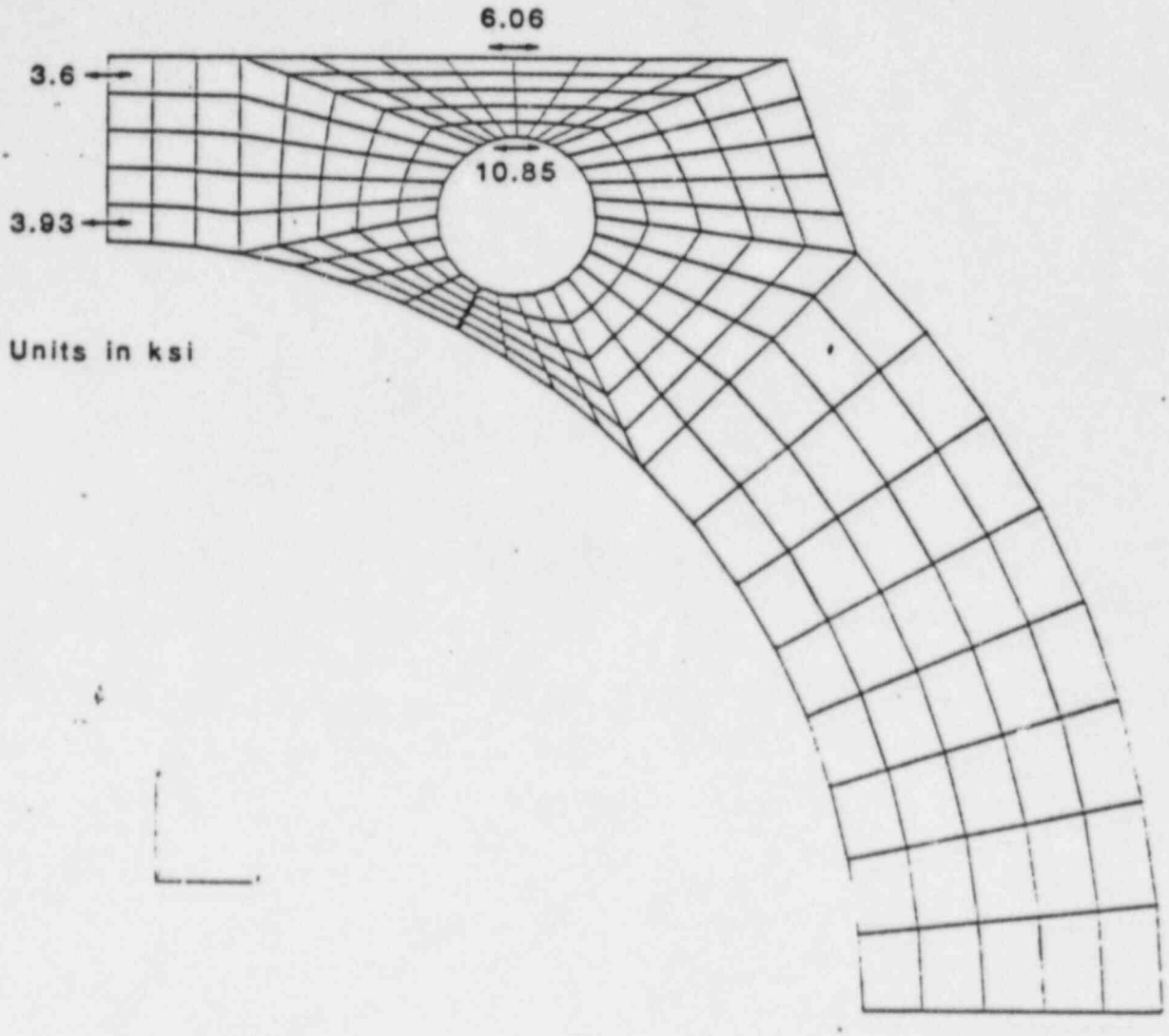

Figure 3-12. Stresses due to radial stress shown in Figure 3-11.

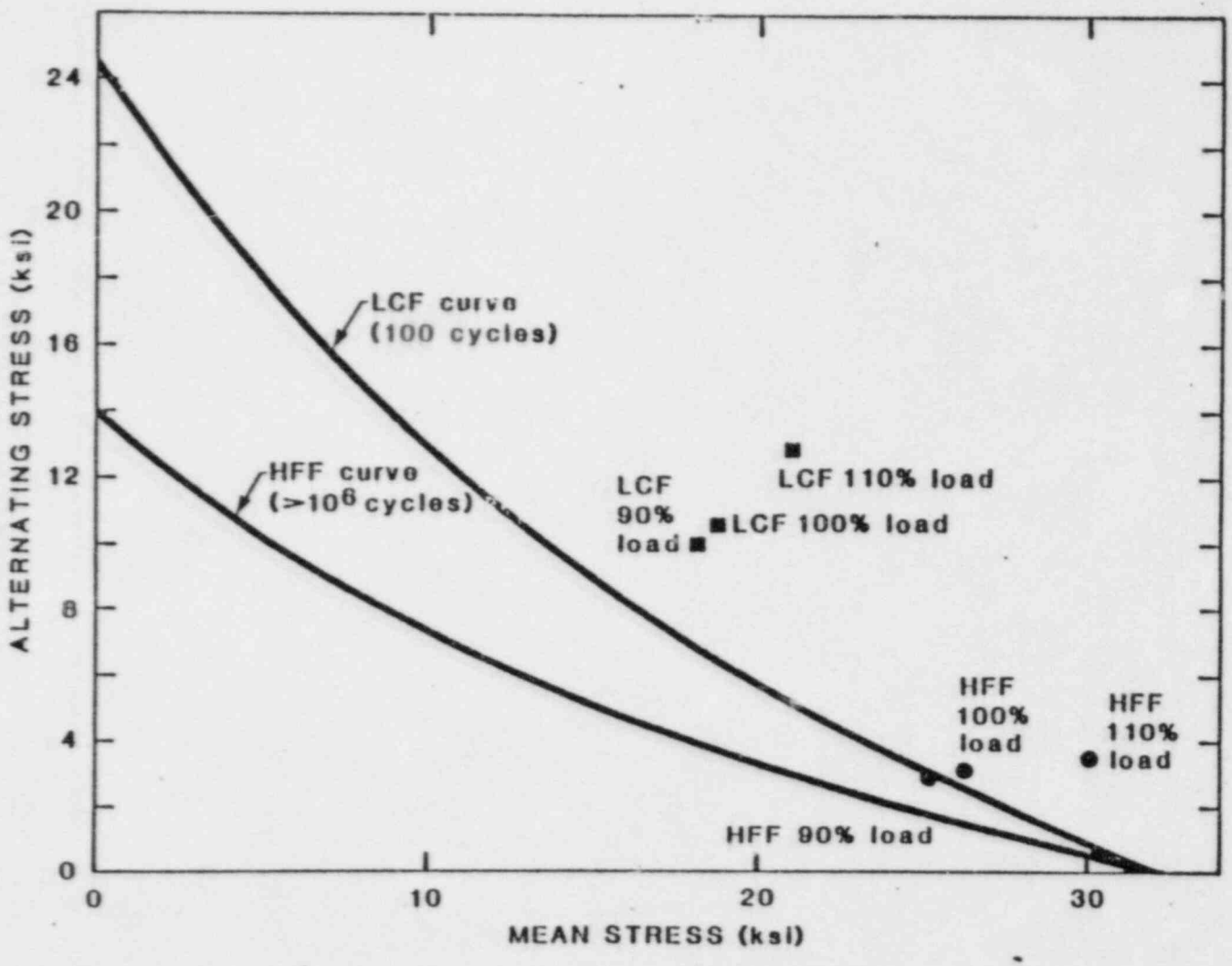

Figure 3-13. Goodman (Smith) diagram for ligament cracking.

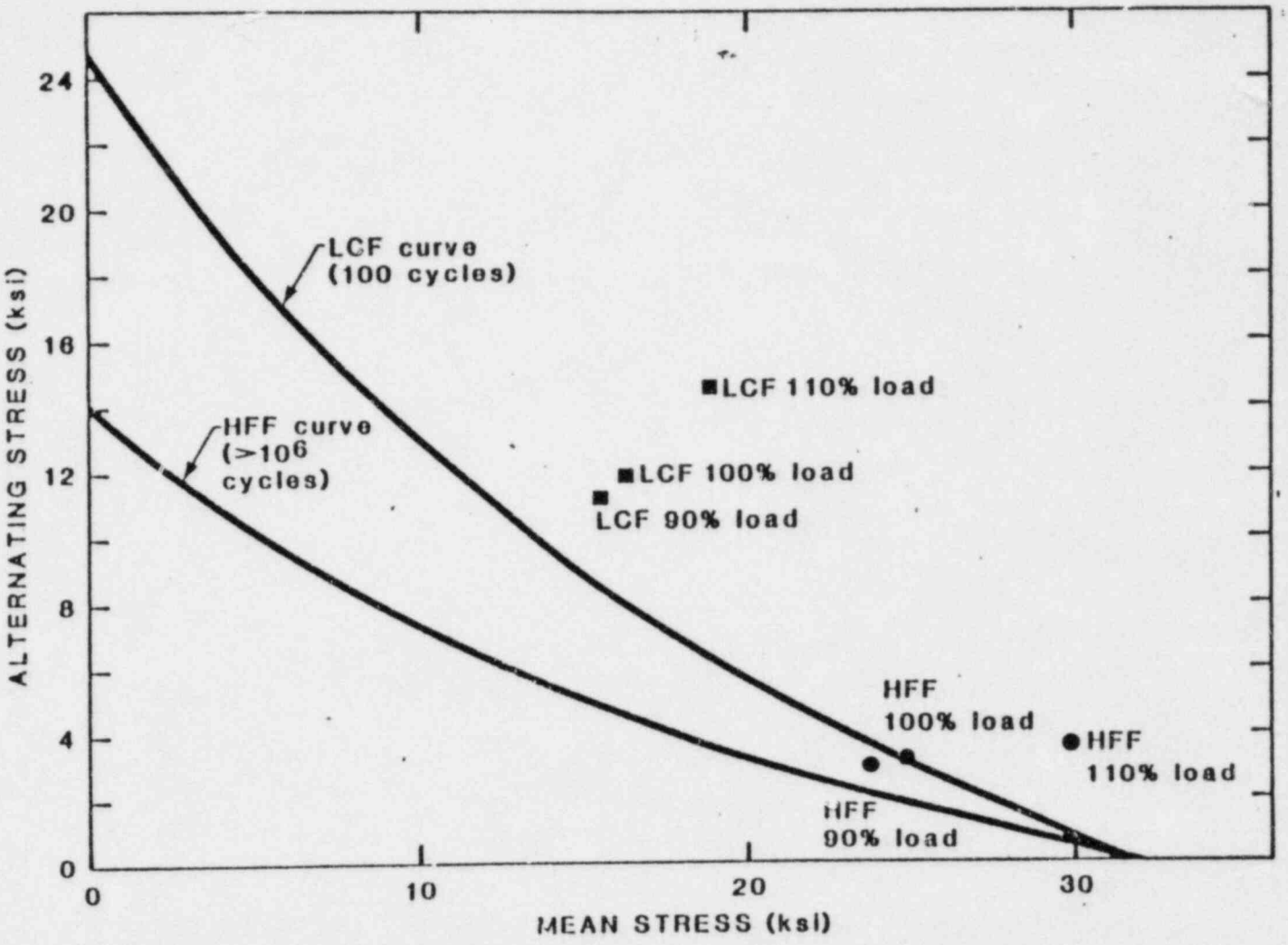

Figure 3-14. Goodman (Smith) diagram for stud-to-stud cracking.

FAA-84-5-4

4.0 FRACTURE AND FATIGUE LIFE EVALUATION

4.1 Block Top Crack Initiation Damage Model

This section analyzes the initiation of block top cracks. A key part of this analysis is the observation that operation at 90% to 100% of rated load is in the fatigue initiation region of the Goodman diagrams for minimum strength cast iron as shown in Figures 3-13 and 3-14. However, the normal variability of material properties could result in no crack initiation under 90% to 100% load operating conditions. The 110% load point is far into the region where initiation is expected with minimum strength cast iron, and it is clearly more damaging relative to 100% load than 100% load is relative to 90% load. At load levels of 80% or less, the minimum acceptable Class 40 material probably will not initiate HFF cracking and will require greater than 100 startup cycles to initiate LCF cracking.

To predict the minimum amount of additional service before cracks are expected to occur between stud holes, it is necessary to consider both LCF and HFF and the current level of damage. If a particular block has operated for a substantial period of time without initiating ligament cracks, this provides an estimate of the minimum LCF and HFF damage required for ligament cracking in that particular block. Since the mean and alternating stresses for initiating ligament cracks and for initiating stud-to-stud cracks in the presence of ligament cracks are almost the same (compare Figures 3-13 and 3-14), at least the same cumulative damage will be required to initiate stud-to-stud cracks after the ligament cracks initiate and grow to a significant depth as was experienced in producing the ligament cracks.

A conservative way to estimate the current level of damage is to divide the time at load and the number of startups to load into categories, i.e., L<70%, 70<L<90%, 90<L<100%, 100<L<105%, 105<L<108%, and L>108%. For LCF, the number of startups that reached the particular load range is tabulated. After an inspection revealing no ligament cracks, subsequent operation without inspection can proceed as long as the number of additional startups in each category are less than the accumulated number at the time of the last inspec-

tion plus the required LOOP/LOCA startup to full power. The number of startups to any lower load level can be increased by reducing the allowable number of startups in a higher load category by an equal number, but not vice-versa.

For HFF, the fatigue damage index from hours in each power level category is computed to estimate the cumulative damage. The approach is similar for fatigue crack propagation and initiation damage, but initiation depends more strongly on stress (n=9.62 from S-n data) than does fatigue crack propagation (conservatively assumed n = 5.37). A cumulative fatigue damage index is computed which accounts for the hours of operation at each power level and the corresponding mean stress and cyclic stress driving the crack at each power level. That is:

$$\text{Fatigue Damage Index} = \sum_i (\text{hours})_i (\Delta\sigma_i)^n \left(\frac{1.73}{1.73-R_i}\right)^n$$

where: $\Delta\sigma_i$ is the stress range $(\sigma_i^{max} - \sigma_i^{min})$ for each i^{th} power level.

R_i is the R-ratio $\equiv \sigma_i^{min}/\sigma_i^{max}$ for i^{th} power level.

$(\text{hours})_i$ is the total expected hours of operation at i^{th} power level.

n is the exponent in the materials fatigue crack growth law (power or Paris law) which describes the stress range dependence of growth rate.

This index accounts for effects of stress range and mean stress on the rate of fatigue crack growth [4-1]. Allowing for the cumulative damage under the specified LOOP/LOCA conditions, the available damage index can be estimated and converted to allowable hours by power level. Figures 3-13 and 3-14 and the cumulative damage calculations strongly suggest that time at or above 100% power is responsible for most of the damage.

Data are available for rough calculation of the total cumulative damage to date in five engines, as in Tables 1-1 through 1-4. Application of the initiation damage index produces the results in Table 4-1. It is evident that the most severely cracked of the SNPS engines (DG103) does have the largest damage index among the SNPS engines. However, the Catawba engine has an even higher damage index without cracking. Furthermore, since the Catawba engine has experienced a cumulative initiation damage index of 106 without cracked ligaments, it should not initiate stud-to-stud cracks before an additional

damage index of 106 is experienced. The sum, 212, is more than double the damage DG103 experienced (87.7) prior to many stud-to-stud cracks, which provides indirect evidence that the properties of block 103 may be inferior to those of Catawba. For reference, the total number of startups is also shown in Table 4-1. These must be broken down by highest load level reached during each start for determing the LCF allowables.

Initiation of ligament cracks in non-nuclear engines is predicted to occur after many load cycles, in low cycle fatigue. These engines typically operate at lower power levels than nuclear engines, where HFF damage is accumulated relatively slowly. In addition the number of startups per running hour is lower. However, in LCF there will be some number of startup cycles to these power levels at which ligament crack initiation is likely. No stud-to-stud cracking is predicted until the number of startup load cycles to typical power levels exceeds twice the number at which ligament cracks initiated.

4.2 Block Top Fatigue Crack Growth Margin Under LOOP/LOCA

The amount of fatigue crack extension that might be expected during a postulated LOOP/LOCA is predicted by cumulative damage analysis of the known experience during the operation of DG103 between 3/11/84 and 4/14/84. The purpose of the calculation is to assess the ability of an engine with cracked ligaments to meet the requirement of at least one LOOP/LOCA after inspection has indicated no stud-to-stud cracking. To make this calculation, the fatigue damage under each power level was computed and added together using the well-known linear cumulative damage approach (presented in Section 4.1) to obtain the total fatigue damage.

A conservative estimate of the fatigue damage index has been computed for conditions under which DG103 was run between 3/11/84 and 4/14/84. A similar calculation was made for the SNPS LOOP/LOCA duty cycle [4-2]. The calculations show that, with the lower bound estimate of stress range and mean stress dependence exponent of n = 5.4, the cumulative damage expected during a LOOP/LOCA is 70% of the damage to which DG103 was exposed between 3/11/84 and 4/14/84. During that period, the maximum crack extension was 4 inches, producing the deepest known crack (5 $^{1}/_{2}$ inches deep) but no operational consequences.

This analysis contains the following conservative assumptions:

- Crack initiation life of the stud-to-stud region is neglected.
- The stress dependence (n) of crack progression rate is assumed to be n=5.37, which was measured at low mean stress (R=0) [4-3] rather than the higher value expected at the high mean stress (R=0.8) calculated to exist in the block during engine operation. Crack growth measurements on ductile iron show that n can increase from 5 to 8.5 as R increases from 0.1 to 0.5. Since the operational R-ratio is 0.8, the exponent n may be much larger. Sensitivity analyses have been performed which show that if the appropriate n is 8.5 for gray cast iron at R=0.8, the fatigue damage index produced during LOOP/LOCA will be about 40% of that introduced into DG103 between 3/11/84 and 4/14/84.
- The materials properties of SNPS block 103 are assumed typical of other blocks even though metallography indicates a potentially inferior microstructure.
- The unusually high temperature conditions which DG103 experienced during the overload excursion, and the possibility of higher temperatures and pressures, have not been included in the cumulative damage assumed to produce the crack extension between studs.
- The lower cylinder pressure and temperatures of specific engines are not accounted for in estimating cumulative damage.

The cast iron block material shows significant variability in ultimate tensile strength and corresponding low cycle fatigue resistance. Casting practice and the presence of tramp elements like lead are particularly important for thick sections. Testing has shown that the strength and ductility of cast iron can be reduced markedly by small percentages of lead which cause a degenerate (Widmanstaetten) graphite microstructure. The development of more extensive cracking in DG103 than in either DG101 or DG102 suggests either inferior material properties and/or more severe service experience. To obtain a preliminary comparison of the materials, a small region of the block tops of engines DG101, DG102, and DG103 was polished and etched to reveal the metallurgical structure. A plastic replica was taken of each etched region and examined in detail in the laboratory microscope. The microstructure of the cast iron from the block of DG103 shows indications of much more extensive

micro-porosity and degenerate graphite. The appearance of the microstructure of DG103 is quite different than that of the engine blocks of DG101 and DG102.

The presence of a degenerate graphite microstructure has been shown to reduce the strength of cast iron significantly [4-4, 4-5]. Specific materials testing is required to quantify any degradation in fatigue or fracture properties of the thick section block casting. A conservative projection of the cracking potential of other engines was obtained by extrapolating the experience of DG103 and assuming that other engine blocks are of equivalent material.

A block with no existing stud-to-stud cracks and material properties sufficiently better than those of DG103 should be able to complete the LOOP/LOCA requirements without any cracks as deep as the 5 $^{1}/_{2}$-inch crack in DG103, while continuing to run normally. Engines with better material or more favorable operating parameters or demands would have less damage. Therefore, these calculations indicate that periodic inspection for radial cracks between the stud holes, in combination with site-specific analysis of operating history, material properties, and operating stress, should assure that block cracks will not grow to a size which will impair the engine's ability to provide the power levels required during a LOOP/LOCA.

4.3 Block Material Properties

The comparison of stresses under full load operation in stud hole regions of the block top with the ultimate strength and fatigue resistance of Class 40 gray cast iron [4-6] shows that fatigue cracking of the ligament region can occur in material with minimum specified properties. On the other hand, if the ultimate strength and fatigue resistance of the block are above average for the Class 40, fatigue crack initiation may not occur without a large number of cold starts and extended operation at or near full power. The cumulative damage index approach provides a method to quantify the effects of alternative engine usage.

Clearly the block top area is not so conservatively designed that cracking will never occur, nor is it so highly stressed that ligament cracks

will always occur. Under these circumstances, the cumulative time/load level/number of cold starts at which cracks develop and the rate at which they progress is strongly dependent upon the materials properties of the specific casting.

Gray cast iron is particularly sensitive to materials properties degradation due to small amounts of tramp elements, like lead. The ultimate tensile strength of thick section castings has been shown to be reduced by as much as 80% of its normal value by the presence of greater than 0.01% lead [4-4, 4-5]. These tramp elements reduce strength and ductility by modifying the normal structure of the graphite flakes to produce degenerate graphite structures with interconnected Widmanstatten (accicular) structure.

The presence of very extensive degenerate graphite microstructures can be identified by conventional metallographic examination. In-situ polishing of block top surfaces, light etching and taking of cellulose acetate (plastic) replicas for microscope examination provides a non-destructive method to detect severely degenerate casting stuctures. Small pieces of block material can also be removed for more detailed metallography and for quantitative chemical analysis to detect the presence of undesirable tramp elements.

4.4 Cam Gallery Cracks

An inspection of the emergency diesel generators at Shoreham revealed crack indications in the cam galleries of all three SNPS engines. These indications were of varying lengths, the longest being 4 1/2 inches long and 0.375 inch deep in DG103. A typical cross-section of the cam gallery is displayed in Figure 4-2, indicating the crack region. TDI installed strain gages on an experimental engine (DSR-46) at the locations of the crack-like defects and recorded the dynamic strains in a running engine. The strain gage data were reduced by TDI to obtain the mean and alternating stresses [4-7]. These stresses are reproduced here in Table 4-2. For the present analysis, stresses obtained at the Gage No. 1 location at 100% load were used.

A fracture mechanics analysis was performed to evaluate the fatigue

crack growth rate of the defect shown in Figure 4-2. The following conventional expression of material fatigue crack growth was used in conjunction with the cyclic and mean stress in the block to compute the fatigue crack growth rate of:

$$\frac{da}{dn} = C\Delta K^n$$

where

$\frac{da}{dn}$ = fatigue crack growth rate, in/cycle

ΔK = cyclic stress intensity factor, ksi $\sqrt{in}$

$C = 3.3 \times 10^{-12}$

$n = 5.37$

The constants C and n were obtained by a linear regression analysis of the fatigue crack growth rate data for gray cast iron [4-3]. A threshold value of zero was assumed for fatigue crack growth. The BIGIF fracture mechanics computer code was used to carry out the fatigue analysis.

For an initial crack of depth of 0.375 inches and length of 4 1/2 inches, the crack growth after 400 hours at full power (5.4×10^6 cycles), was predicted to be 0.034 inch in depth by 0.006 inch in length.

Section 4 References

4-1 A. Yuen, et al., "Correlations Between Fracture Surface Appearance and Fracture Mechanics Parameters for Stage II Fatigue Crack Propagation in Ti-6 AC-4V, Metallurgical Transactions 5, p. 1833, August 1984.

4-2 Stone and Webster Letter of 12/15/83 to LILCO, Subject: Two-Year Operating Cycle Emergency Diesel Generators SNPS.

4-3 C. F. Walton and T. J. Opar, Iron Castings Handbook, Iron Castings Society, Inc., 1981.

4-4 C. E. Bates and J. F. Wallace, "Trace Elements in Gray Iron," American Foundrymen's Socienty, Report of Research Project.

4-5 C. E. Bates, "Effect and Neutralization of Trace Elements in Gray and Ductile Iron," Ph.D Thesis, Case Western Reserve University (1968).

4-6 L. E. Tucker and D. R. Olberts, "Fatigue Properties of Grey Cast Iron", SAE Paper No. 690471, SAE Transactions, Vol. 78, 1969.

4-7 Dean T. Ripple, "R4-L6 Cam Gallery Strain Gage Test," Transamerica Delaval Inc., Engine and Compressor Division, R and D Report, FR-01-1983, Rev. June 21, 1983.

TABLE 4-1

CUMULATIVE DAMAGE IN NUCLEAR ENGINES TO MAY-1984

	Shoreham Engines				
	DG101	DG102	DG103	Catawba 1a	Grand Gulf 1
Total Number of Startups	709*	490	401	120	586*
Cumulative Initiation Damage Index (n=9.6)	80.5	83.5	87.7	106.1**	39.8†

For reference, the cumulative initiation damage index (n=9.6) for one LOOP/LOCA is 4.7.

* Includes 300 factory starts to 67% of full load.
** Includes 201 hours at unknown power level, assumed to be 50%.
† Includes 442 hours at unknown power level, assumed to be 50%.

TABLE 4-2

MEAN AND ALTERNATING STRESSES (FROM REFERENCE 4-5)

Gage No.		Stress - psi			
		0 Load	50% Load	100% Load	110% Load
1	Mean	-1530	-612	2176	2950
	Alt.	1216	602	1239	1350
2	Mean	-714	-646	1088	2275
	Alt.	1413	637	881	1200
3	Mean	-4363.5	-1802	2357.5	3475
	Alt.	2104.5	1816	1036.5	815

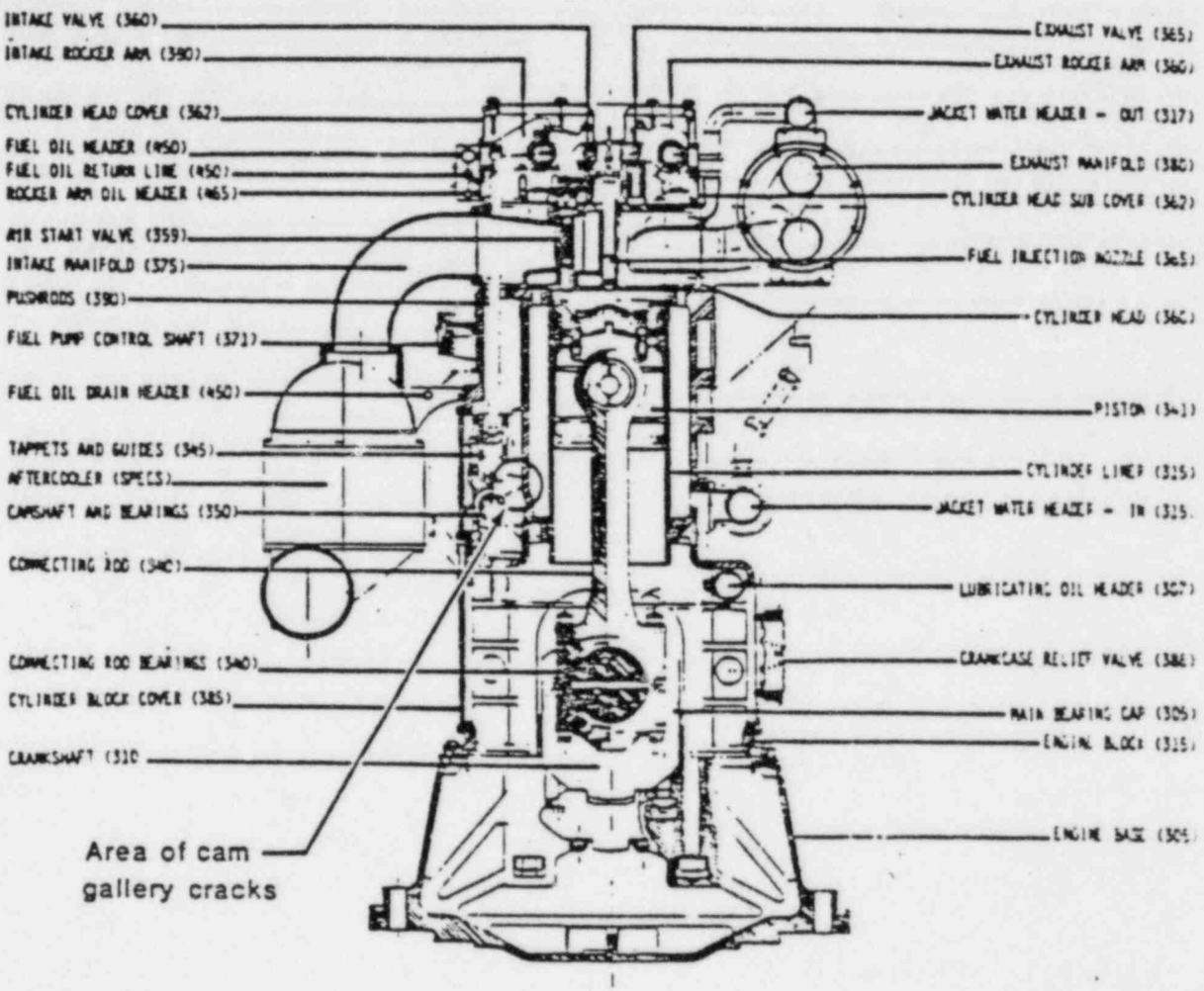

Figure 4-1. Cam gallery geometry.

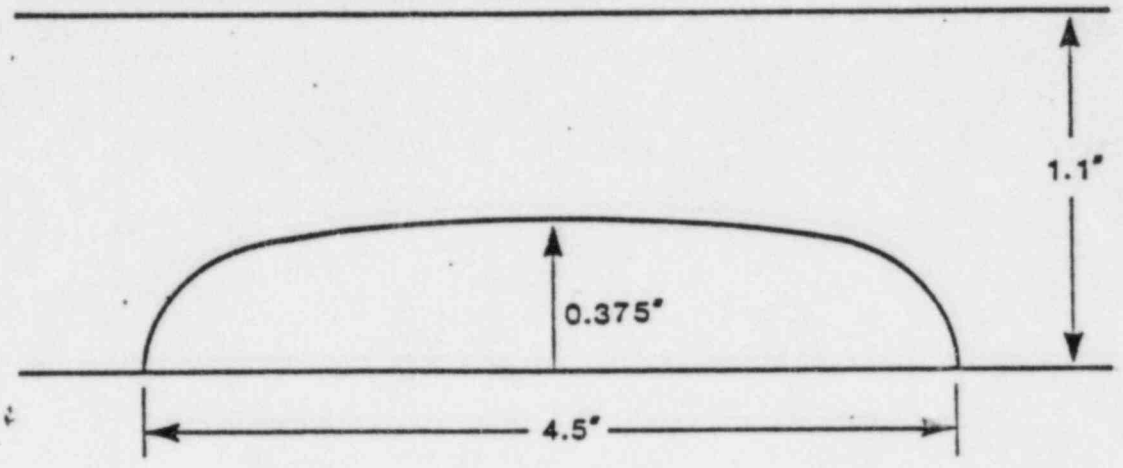

Figure 4-2. Cam gallery crack shape.

5.0 CONCLUSIONS AND RECOMMENDATIONS

Review of operating experience with TDI R-4 and RV-4 cylinder blocks indicates that precautions are necessary to avoid the potential consequences of block top cracking between stud holes of adjacent cylinders. The results of strain gage testing, combined with two-dimensional analytical models of the block top and liner and cumulative damage estimates, provide the following conclusions and recommendations:

1. Initiation of cracks in the ligament between stud hole and liner counterbore is predicted to occur after accumulating operating hours at high load and/or engine starts to high load. These cracks are benign because the cracked section is fully contained between the liner and the region of the block top outside the stud hole circle. Field experience is consistent with both the prediction of ligament cracking and the lack of immediate consequences.

2. The presence of ligament cracks between stud hole and liner counterbore increases the stress and the probability of cracking between the stud holes of adjacent cylinders such that stud-to-stud cracks are predicted to initiate after additional operating hours at high load and/or engine starts to high load. The deepest measured crack in this region (5 $^{1}/_{2}$-inch depth) did not degrade engine operation or result in stud loosening.

3. The apparent rate of propagation of cracks between stud holes in the DG103 block at SNPS, when compared with the LOOP/LOCA requirements, indicates that blocks with ligament cracks (e.g., DG101 and DG102) are predicted to withstand a LOOP/LOCA event with sufficient margin provided that: (1) inspection shows no stud-to-stud cracks detectable between heads, and (2) the specific block material of DG103 is shown to be sufficiently less resistant to fatigue than typical gray cast iron, Class 40.

4. The block tops of engines that have operated at or above rated load should be inspected for ligament cracks. Engines such as those at Catawba and Grand Gulf that are found to be without ligament cracks can be operated without additional inspection for combinations of load, time, and number of starts that produce

less expected damage than the cumulative damage prior to the latest inspection. The allowable engine usage without repeated inspection can be determined from cumulative damage analysis.

5. The blocks of engines that have been operated at or above rated load without subsequent inspection of the block top should conservatively be assumed to have cracked ligaments for the purpose of defining inspection intervals.

6. For blocks with known or assumed ligament cracks, the absence of detectable cracks between stud holes of adjacent cylinders should be established by eddy current inspection before returning the engine to emergency standby service after any period of operation other than no load. If crack indications are found, removal of the adjacent heads and detailed inspection and evaluation of the block top are necessary. In addition, it is necessary to ensure that the microstructure of the block top does not indicate inferior mechanical properties.

7. Engines that operate at lower maximum pressure and temperature than the SNPS engines (e.g., San Onofre) may have increased margins against block cracking that could allow relaxation of block top inspection requirements. Modifications to other parameters such as increased liner-to-block radial clearance will reduce stresses, and site specific analyses of such modification could also permit relaxation of inspection requirements.

Appendix:

COMPONENT DESIGN REVIEW

TASK DESCRIPTION

CYLINDER BLOCK
Part No. 03-315A

Classification A
Completion Date 3/20/84

PRIMARY FUNCTION: The cylinder block comprises the framework of the liquid cooled engine and provides passage and support for the cylinder liner. The block must provide cooling water passages, provide bores to support the cam shaft assembly, and react the dynamic loads from the cylinder firing pressure and valve assemblies. For the RV engines, the cylinder block is interconnected with an engine crankcase which supports the camshaft and associated bearings. Although these are separate parts, their generic function is similar to the cylinder block of the R-48 engines and will therefore be evaluated as a unit. The liner itself forms the walls of the combustion chamber containing the high temperature gas pressure and must provide a guide for the piston motion while reacting skirt side forces without excessive wear or scuffing.

FUNCTIONAL ATTRIBUTES:

1. The cam gallery bearing supports must be designed to maintain concentricity during service and have sufficient structural strength to react the cam/valve train loads without fatigue cracking.

2. The support of the cylinder liner must maintain tight seals, react pressure and stud loads without unacceptable distortion and maintain sufficient load distribution to preclude excessive cracking in the liner counterbore (landing) due to combined thermal, gas pressure and preloaded stud induced states of stress. The cylinder head stud thread configuration is important in determining stress concentrations and stress distributions.

3. The cylinder liner itself must be sufficiently hardened to resist unacceptable wear associated with piston ring action and maintain adequate contact with the block counterbore to prevent high cycle contact stress and fretting. In addition, the compression of the head to the cylinder liner must be sufficient to avoid axial fretting of the liner within the counterbore but not so great as to cause failures of the cylinder block liner landing.

4. The cooling water distribution within the block must be sufficient to preclude overheating of the block and liner and must maintain proper flow conditions to minimize or avoid cavitation or corrosion damage to the liner.

SPECIFIED STANDARDS: None

EVALUATION:

1. Review information concerning previous cracking and distortion of the cylinder block and liners of the R48 and RV engines.

2. Review liquid penetrant inspections of cylinder block in the head stud and liner counterbore regions of the SNPS DSR-48 engines.

3. Evaluate the steady state and alternating stresses in the liner landing/head stud region and compare these to yield and endurance limits for appropriate materials. This examination must consider variations in head stud thread geometries and preload torques.

4. Evaluate the state of stress in the liner in the landing/axial seal region due to gas pressures, thermal growth and head clamping forces and compare to normal fatigue properties for liner material.

5. Evaluate critical flaw size and rate of crack growth considering combined head stud loads and thermal stresses for cracks located between head stud holes and cylinder block counterbore diameter.

6. Evaluate critical flaw size and rate of crack growth for cracks eminating from the corner of the cylinder block landing and counterbore diameter.

7. Evaluate the loading produced on the bearing supports in the cam gear gallery and verify the structural adequacy of the design.

8. Review the inspection of the sampled SNPS cylinder lines following 100 hours at 100% load for evidence of unacceptable scuffing, corrosion, cracking, or scoring.

9. Review information provided on TER DR-220.

REVIEW TDI ANALYSES:

1. Review any TDI analyses which consider stresses created in the liner counterbore area and any design changes which relate to geometry or material.

INFORMATION REQUIRED:

1. Manufacturer's drawings of R48 and RV cylinder blocks and liners, including material specifications and historical design changes.

2. Gas pressures and temperatures for R48 and RV engine designs.

3. Cylinder head stud drawings and torque specifications.

4. Cylinder head stud drawings showing design changes.

5. Liquid penetrant inspection of cylinder block counterbore (landing) on SNPS engines.

6. Cam shaft loads due to rocker arms, pushrods and valve springs.